

**Fluorescence measured  
in situ as a proxy of  
CDOM absorption and  
DOC concentration in the  
Baltic Sea\***

OCEANOLOGIA, 52 (3), 2010.  
pp. 431–471.

© 2010, by Institute of  
Oceanology PAS.

**KEYWORDS**

CDOM absorption  
DOC concentration  
Baltic Sea

PIOTR KOWALCZUK\*  
MONIKA ZABŁOCKA  
SŁAWOMIR SAGAN  
KAROL KULIŃSKI

Institute of Oceanology,  
Polish Academy of Sciences,  
Powstańców Warszawy 55, PL-81-712 Sopot, Poland;

e-mail: piotr@iopan.gda.pl

\*corresponding author

Received 20 April 2010, revised 27 July 2010, accepted 9 August 2010.

**Abstract**

This study presents results from field surveys performed in 2008 and 2009 in the southern Baltic in different seasons. The main goal of these measurements was to identify the empirical relationships between DOM optical properties and DOC. CDOM absorption and fluorescence and DOC concentrations were measured during thirteen research cruises. The values of the CDOM absorption coefficient at 370 nm  $a_{\text{CDOM}}(370)$  ranged from  $0.70 \text{ m}^{-1}$  to  $7.94 \text{ m}^{-1}$ , and CDOM fluorescence intensities (ex./em. 370/460)  $I_{\text{FI}}$ , expressed in quinine sulphate equivalent units, ranged from 3.88 to 122.97 (in filtered samples). Dissolved organic carbon (DOC) concentrations

---

\* This study was funded by the Polish Ministry of Science and Higher Education through grant No. NN 306-2942-33 for the research project entitled ‘Spectral properties of CDOM absorption and fluorescence and their relationship with Dissolved Organic Carbon concentration in the Baltic Sea’. The principle investigator was Piotr Kowalczuk. The research infrastructure, including access to the research vessel r/v ‘Oceania’, was provided by the Institute of Oceanology, Polish Academy of Sciences, Sopot, Poland. Partial support for this study was also provided by the project Satellite Monitoring of the Baltic Sea Environment – SatBałtyk, co-founded by the European Union through European Regional Development Fund contract No. POIG 01.01.02-22-011/09.

ranged from 266.7 to 831.7  $\mu\text{M C}$ . There was a statistically significant linear relationship between the fluorescence intensity measured in the filtered samples and the CDOM absorption coefficient  $a_{\text{CDOM}}(370)$ ,  $R^2 = 0.87$ . There was much more scatter in the relationship between the fluorescence intensity measured in situ (i.e. in unprocessed water samples) and the CDOM absorption coefficient  $a_{\text{CDOM}}(370)$ , resulting in a slight deterioration in the coefficient of determination  $R^2 = 0.85$ . This indicated that the presence of particles could impact fluorometer output during in situ deployment. A calibration experiment was set up to quantify particle impact on the instrument output in raw marine water samples relative to readings from filtered samples. The bias calculated for the absolute percentage difference between fluorescence intensities measured in raw and filtered water was low ( $-2.05\%$ ), but the effect of particle presence expressed as the value of the RMSE was significant and was as high as 35%. Both DOM fluorescence intensity (in raw water and filtered samples) and the CDOM absorption coefficient  $a_{\text{CDOM}}(370)$  are highly correlated with DOC concentration. The relationship between DOC and the CDOM absorption coefficient  $a_{\text{CDOM}}(370)$  was better ( $R^2 = 0.76$ ) than the relationship between DOC and the respective fluorescence intensities measured in filtered and raw water ( $R^2 = 0.61$  and  $R^2 = 0.56$ ). The seasonal cycle had an impact on the relationship between DOC and CDOM optical properties. The hyperbolic relationships between  $a_{\text{CDOM}}(370)$  vs. carbon-specific absorption coefficient  $a^*_{\text{CDOM}}(370)$ , and  $I_{\text{F1}}$  vs. the ratio of fluorescence intensity to organic carbon concentration  $I_{\text{F1}}/\text{DOC}$  were very good. The discharge and mixing of riverine waters is a primary driver of variability in DOC and CDOM optical properties in the surface waters of the southern Baltic Sea, since all the parameters considered are negatively correlated with salinity. It was found that there was a positive trend of increasing values of DOM optical parameters with salinity increase (within a range of 8–12) in deep water below the permanent pycnocline. Evidence is also presented to show that late-summer photodegradation was responsible for the depletion of CDOM fluorescence intensities in the mixed layer above the seasonal thermocline. It was further demonstrated that the DOC concentration increases in the stagnant waters of the Baltic Sea deeps. The Integrated Optical-Hydrological Probe, which registers high-resolution vertical profiles of salinity, temperature, CDOM and the optical properties of water, confirmed that DOM optical proxies can be used in studies of DOM biogeochemical cycles in the Baltic Sea.

## 1. Introduction

The cycling of dissolved organic matter (DOM) is a key but as yet underdeveloped element of global climate models. Improvements in and the validation of global climate models depend on high spatial and temporal resolution of dissolved organic carbon (DOC) concentration data collected in the field. Identifying relationships between DOM optical properties and DOC concentrations and using optical signatures as proxies for DOC can increase the spatial and temporal resolution of field measurements of DOC distribution in the oceans, thus contributing to a better understanding of the

global carbon cycle. The largest reservoir of organic carbon in the oceans is the Dissolved Organic Matter (DOM) (Hansell & Carlson 1998). About 97% of all organic carbon in the sea is bound up in DOM, with an estimated 685 Gt as Dissolved Organic Carbon (DOC) (Hansell & Carlson 2001).

CDOM is the primary absorber of sunlight and is a major factor determining the optical properties marine and oceanic waters. It also affects directly the availability and the spectral quality of light in aquatic environments. Moreover, the absorption of light by CDOM has an influence on both the inherent and apparent optical properties of seawater. Together with light absorption by pure water, phytoplankton pigments, organic and inorganic matter suspended in marine waters, and scattering processes, CDOM absorption shapes the spectral optical properties of sea water and light fields in water columns (Morel & Prieur 1977, Sathyendranath (ed.) 2000, Blough & Del Vecchio 2002). This is why the optical properties of CDOM have been the subject of studies since the inception of ocean optics as a marine science discipline (Jerlov 1976). CDOM absorption decreases exponentially towards longer wavelengths and can be described by the exponential equation (Kirk 1994)

$$a_{\text{CDOM}}(\lambda) = a_{\text{CDOM}}(\lambda_0)e^{-S(\lambda-\lambda_0)}, \quad (1)$$

where  $a_{\text{CDOM}}(\lambda)$  is the absorption coefficient at wavelength  $\lambda$ ,  $\lambda_0$  is the reference wavelength and  $S$  is the slope coefficient (the exponential decrease of the absorption spectrum over a given wavelength range). These parameters describe CDOM quantitatively and can be used to estimate the entire absorption spectrum from equation (1) if absorption at the fixed (reference) wavelength and  $S$  are known.

The fluorescent properties of CDOM have been known for a long time (Duursma 1965), and fluorescence signals have been used to estimate CDOM in marine waters. Many investigators have observed a linear relationship between fluorescence and absorption (Ferrari & Tassan 1991, Hoge et al. 1993b, Vodacek et al. 1997, Ferrari & Dowell 1998, Ferrari 2000), and that between fluorescence intensity and the CDOM absorption coefficient was used to estimate the absorption of soluble material during in situ deployments of fluorometers on moorings, or with profiling probes or using lidar systems mounted on various platforms (e.g. Hoge et al. 1993a, Conmy et al. 2004, Belzile et al. 2006).

Interest in CDOM and its characterization has grown recently for several reasons: i) remote sensing of ocean colour is related to organic carbon cycling (Blough & Del Vecchio 2002); ii) possible interference with remote sensing measurements of chlorophyll as an indicator of primary productivity; iii) air-sea exchange of important trace gases, namely CO, CO<sub>2</sub> and COS;

iv) the formation of reactive oxygen species and their potential impact on biological processes and geochemical cycling; v) as a tracer of riverine input of organic carbon to the ocean and carbon cycling in coastal waters; vi) the attenuation of ultraviolet light in surface waters. Quantitative descriptions of the dynamics and variability of CDOM optical properties are often required, particularly in coastal waters, in order to accurately predict light penetration and subsequently, for example, primary productivity.

Semi-analytical algorithms for estimating the inherent optical properties of sea waters from ocean colour satellite imagery produce values of chlorophyll concentrations together with CDOM and particulate absorption coefficients (Garver & Siegel 1997, Maritorena et al. 2002). These algorithms are applied to produce maps at basin-wide scales and of the global distribution of CDOM absorption and its seasonal variability (Siegel et al. 2002). The application of semi-analytical algorithms for observations of CDOM absorption by ocean colour imagery has also enabled explanations of the differences in chlorophyll *a* retrievals resulting from the application of empirical algorithms in various oceanic basins (Siegel et al. 2005b), and thus, a reassessment of the principal theoretical assumptions of ocean optics (Siegel et al. 2005a). In oceanic coastal areas and semi-enclosed seas, which are optically complex case 2 waters, empirical band ratio algorithms are often used to estimate CDOM absorption and its impact on light transmission through the water column in the UV and visible spectra (Kahru & Mitchell 2001, D'Sa & Miller 2003, Johannessen et al. 2003, Kowalczyk et al. 2005, Fichot et al. 2008, Mannino et al. 2008).

The application of ocean colour remote sensing to estimate CDOM optical properties together with models of their modification through photochemical reactions (Johannessen & Miller 2001) provides an opportunity to study CDOM mineralization over vast areas of oceanic basins (Bélanger et al. 2006, Del Vecchio et al. 2009). These studies contribute directly to carbon cycle research calculations of CO<sub>2</sub> exchange between the ocean and the atmosphere.

In situ and remote sensing measurements of the optical properties of CDOM are relatively easy to perform, thus making use of CDOM absorption or fluorescence as a proxy for DOC concentration very attractive. Although CDOM contributes approximately 20% to the total DOC pool in the open ocean and up to 70% in coastal areas (Coble 2007), a direct link establishing a global relationship between CDOM and DOC has not yet been identified. CDOM is a complex mixture of heterogeneous organic compounds, each having individual optical properties. Therefore, the estimation of the universal bulk carbon-specific CDOM absorption coefficient  $a^*_{\text{CDOM}}(\lambda)$ , defined as the ratio  $a_{\text{CDOM}}(\lambda)/\text{DOC}$ , seems almost

impossible (Woźniak & Dera 2007). Another aspect that complicates a global DOC-CDOM relationship is that processes responsible for the production, decomposition and distribution of bulk DOC and CDOM components are decoupled in oceanic systems.

In oligotrophic subtropical gyres and central open ocean areas not in close proximity to terrestrial influence, there is a significant time phase shift between maximum DOC concentration produced by phytoplankton blooms and maximum CDOM absorption (Nelson et al. 1998, Siegel et al. 2002). Additionally, in surface waters, CDOM absorption is quickly diminished by intensive photobleaching (Vodacek et al. 1997, Johannessen et al. 2003). Below the mixing zone, there is usually an increase in CDOM absorption in contrast to the decrease in DOC levels (Nelson et al. 2007). A strong correlation between both  $a_{\text{CDOM}}(\lambda)$  and DOC exists only in areas where the variability of each parameter is controlled by the mixing of fresh and oceanic waters. Several studies have reported a good correlation between  $a_{\text{CDOM}}(\lambda)$  and DOC in coastal areas (Green & Blough 1994, Vodacek et al. 1995 and 1997, Ferrari et al. 1996, Ferrari 2000, Chen et al. 2002, Rochelle-Newall & Fisher 2002a, Del Vecchio & Blough 2004). However, it was later demonstrated that the optical properties of CDOM are not conservative, and they change because of CDOM degradation processes such as photochemical reactions and bacterial grazing, which also lead to seasonal variability in  $a_{\text{CDOM}}(\lambda)$  vs. DOC relationships in coastal oceans (Vodacek et al. 1997, Rochelle-Newall & Fisher 2002a, Del Vecchio & Blough 2004, Mannino et al. 2008). These local and highly-variable relationships are valuable for studying carbon cycling in coastal areas because they permit the application of ocean colour remote sensing to capture synoptic DOC distribution at high spatial and temporal resolution (e.g. Del Castillo & Miller 2008, Mannino et al. 2008).

The empirical relationships between the optical properties of CDOM and DOC have already been the subject of investigation in the Baltic Sea (Nyquist 1979, Ferrari et al. 1996, Stedmon et al. 2000), and the results published indicate their seasonal variation. These results are based on data collected during several field surveys that were generally conducted during one seasonal cycle. The main objective of the current study was to reassess these relationships over a longer observation period of at least two seasonal cycles, and to use commercial fluorimeters to take in situ measurements of the dynamics of CDOM optical properties at a higher spatial and temporal resolution than is achieved with the traditional water sampling approach. An additional objective was to investigate the relationships between salinity, temperature, CDOM optical properties and organic carbon distribution based on data from traditional water sampling and high spatial resolution

vertical profiles of these parameters registered with the Integrated Optical-Hydrological probe to indicate potential areas of the sources and losses of both CDOM and DOC in the study area.

## 2. Methods

### 2.1. Study area

Conducted in the southern Baltic Sea, the study was based on measurements of 476 absorption spectra of CDOM, CDOM fluorescence and Dissolved Organic Carbon (DOC) concentrations collected for a research project focused on the spectral properties of CDOM absorption and fluorescence. The field work was conducted during a pilot study in May 2004 and over a period of two years during the main phase of the project in 2008 and 2009. Logistical support was provided by a long-term bio-optical observation programme in the Baltic Sea carried out by the Institute of Oceanology of the Polish Academy of Sciences. Water samples

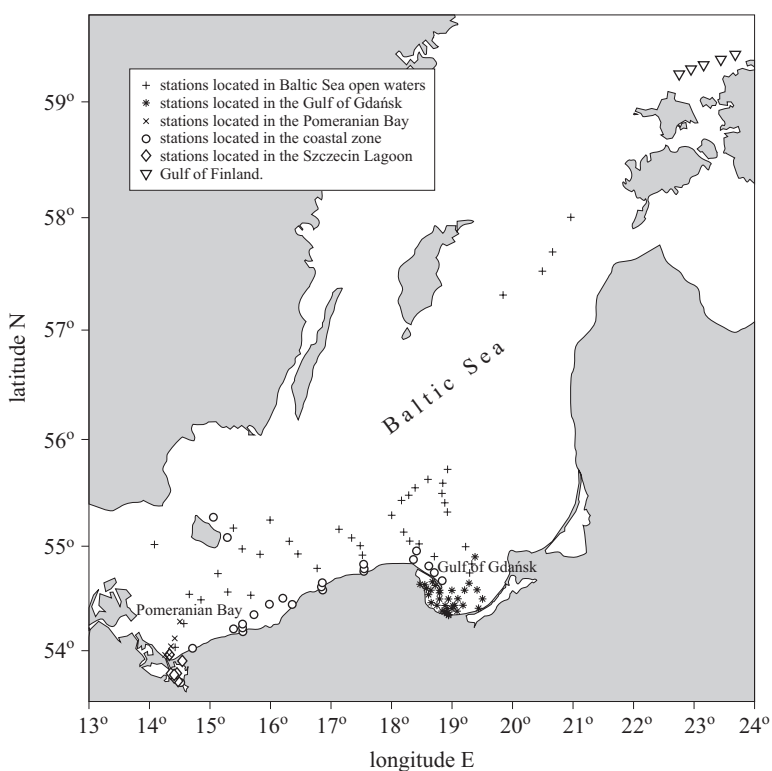


**Figure 1.** Distribution of the sampling stations in the Baltic Sea during the field survey in 2008–2009

**Table 1.** Dates, number of stations sampled, number of samples collected and parameters measured during cruises made for this study

Dates of cruises	Number of stations	Number of samples	Parameters measured	Region
15–25 May 2004 (pilot study)	50	71	$a_{\text{CDOM}}(\lambda)$ , CTD, DOC	southern Baltic Proper, Gulf of Gdańsk
30 Jan.–08 Feb. 2008	24	32	$a_{\text{CDOM}}(\lambda)$ , CTD, DOC $I_{\text{Fl\_CDOM}}$	southern Baltic Proper, Gulf of Gdańsk
01–11 March 2008	30	35	$a_{\text{CDOM}}(\lambda)$ , CTD, DOC, $I_{\text{Fl\_CDOM}}$	southern Baltic Proper, Gulf of Gdańsk, Pomeranian Bay
11–18 April 2008	25	29	$a_{\text{CDOM}}(\lambda)$ , CTD, DOC, $I_{\text{Fl\_CDOM}}$	southern Baltic Proper, Gulf of Gdańsk
06–14 May 2008	31	33	$a_{\text{CDOM}}(\lambda)$ , CTD, DOC, $I_{\text{Fl\_CDOM}}$	southern Baltic Proper, Gulf of Gdańsk
01–09 Sept. 2008	29	30	$a_{\text{CDOM}}(\lambda)$ , CTD, DOC, $I_{\text{Fl\_CDOM}}$	southern Baltic Proper, Gulf of Gdańsk, Pomeranian Bay, Szczecin Lagoon
25–29 Nov. 2008	19	21	$a_{\text{CDOM}}(\lambda)$ , CTD, DOC, $I_{\text{Fl\_CDOM}}$	Gulf of Gdańsk
04–12 March 2009	20	28	$a_{\text{CDOM}}(\lambda)$ , CTD, DOC, $I_{\text{Fl\_CDOM}}$	Gulf of Gdańsk, Gotland Basin
02–04 April 2009	12	12	$a_{\text{CDOM}}(\lambda)$ , CTD, DOC,	Baltic Proper, Gulf of Finland
15–28 April 2009	38	51	$a_{\text{CDOM}}(\lambda)$ , CTD, DOC, $I_{\text{Fl\_CDOM}}$	southern Baltic Proper, Gulf of Gdańsk
20–28 May 2009	36	54	$a_{\text{CDOM}}(\lambda)$ , CTD, DOC, $I_{\text{Fl\_CDOM}}$	southern Baltic Proper, Gulf of Gdańsk, Pomeranian Bay, Szczecin Lagoon
07–16 Sept. 2009	40	56	$a_{\text{CDOM}}(\lambda)$ , CTD, DOC, $I_{\text{Fl\_CDOM}}$ in situ, ac-9	southern Baltic Proper, Gulf of Gdańsk
06–10 Oct. 2009	21	24	$a_{\text{CDOM}}(\lambda)$ , CTD, DOC, $I_{\text{Fl\_CDOM}}$ in situ, ac-9	southern Baltic Proper, Gulf of Gdańsk

Fluorescence measured in situ as a proxy of CDOM absorption ...

were collected during 13 cruises in the southern Baltic Proper (Figure 1) in the months of February to May and September to November. Details of the cruises, including dates, number of stations sampled, parameters measured and the number of samples collected are presented in Table 1. The geographical coverage of the samples included the Gulf of Gdańsk, the Pomeranian Bay, the Szczecin Lagoon, Polish coastal waters and the open sea (the Baltic Proper). The coastal sites in the Gulf of Gdańsk and the Pomeranian Bay are under the direct influence of two major river systems, the Vistula and the Odra, which drain the majority of Poland.

The Baltic Sea has high concentrations of CDOM that come from the high input of fresh water from a large drainage area and limited water exchange with the North Sea; thus, the optical effects of CDOM are particularly relevant in this area. The southern Baltic Sea is located in the temperate climatic zone. Maximum freshwater runoff occurs in April/May and coincides with the spring phytoplankton bloom, initiated by the stabilization of the water column and increased surface light. The fresh water carries both high concentrations of CDOM and substantial loads of inorganic nutrients. The nutrients enhance the spring bloom, and in combination with the CDOM, cause an increase in light attenuation. In the summer, local coastal upwelling events caused by Ekman transport, as well as periodic summer floods, affect the optical properties in the coastal zone and bays. In the winter, wind-driven mixing, the vertical thermohaline circulation, reduced biological activity and reduced riverine outflow all result in clearer surface waters (Sagan 1991, Olszewski et al. 1992, Kowalczyk 1999). CDOM has a significant influence on the spectral properties of the apparent optical properties of Baltic Sea water. A high CDOM concentration causes a shift in the maximum solar radiation transmission towards longer wavelengths relative to clear oceanic water (Darecki et al. 2003, Kowalczyk et al. 2005).

## 2.2. Optical properties of CDOM

Water samples for determining CDOM absorption, CDOM fluorescence and DOC concentration were collected at fixed depths with Niskin bottles. The majority of samples were collected from the photic zone. Water samples for CDOM underwent a two-step filtration process. The first filtration was through acid-washed Whatman glass fibre filters (GF/F, nominal pore size  $0.7 \mu\text{m}$ ). The water was then passed through Sartorius  $0.2 \mu\text{m}$  pore cellulose membrane filters to remove fine-sized particles. Spectral absorption by CDOM was measured in the laboratory on board r/v 'Oceania' using a double-beam Unicam UV4-100 spectrophotometer with a 5-cm quartz cell in the spectral range of 200–700 nm. MilliQ water was used as the reference



for all measurements. The absorption coefficient  $a_{\text{CDOM}}(\lambda)$  was calculated using the following equation:

$$a_{\text{CDOM}}(\lambda) = \frac{2.303A(\lambda)}{l}, \quad (2)$$

where  $A(\lambda)$  is the absorbance (optical density) and  $l$  the path length.

Following the recommendation by Stedmon et al. (2000), the spectral slope of the absorption spectrum  $S$  was calculated by applying the simple exponential model to fit the offset-corrected absorption spectrum in the spectral range  $350 \leq \lambda \leq 550$  nm for most of the samples collected. This method of spectral slope calculation is less dependent on the spectral range used. The short wavelength limit was applied to reduce the possible effect of absorption due to the presence of lignin sulphates (Nyquist 1979), which is observed in some samples as a small bump in the spectral range 260–310 nm. In most cases the upper wavelength was between 550 nm and 600 nm. For wavelengths longer than 600 nm, the absorbance signal was usually low and the spectrum had lost its linear properties in the semi-logarithmic scale. The offset is the effect of residual scattering and was removed by subtracting the scattering component from the spectrum on the assumption that scattering is independent of wavelength. The average absorbance in the spectral range 650–700 nm, where the linear model was not obeyed, enabled assessment of this component, which was then subtracted from the whole spectrum.

CDOM fluorescence was measured with a MicroFlu-CDOM fluorometer (TRIOS GmbH, Germany), which is suitable for in situ measurements without the prior filtration of the water. The MicroFlu-CDOM fluorometer uses UV-LED in pulse mode as the excitation light source. The maximum of the excitation light spectrum is 370 nm. A small percentage of light is reflected by the dichroitic beam splitter and is used as the reference signal for calculating the excitation energy. The fluorometer excites samples of a small volume of water at the front of the optical window at a focal length of 15 mm. It uses a photo-diode with an interference filter as the light detector. The maximum emission of the light detector is set at 460 nm. Specially developed circuitry eliminates the influence of ambient light. The MicroFlu-CDOM fluorometer was calibrated by the manufacturer annually during the deployment period (2008–2009). The fluorescence intensity of the CDOM contained in the water samples was recorded in quinine sulphate equivalent units – QSE. This is an apparent unit that relates the intensity of CDOM to the fluorescence intensity of a standard compound with well-known fluorescence properties, which is usually a concentration of a solution of quinine sulphate dehydrate (Fluka 22640) in 0.05 M sulphuric acid in  $\mu\text{g dm}^{-3}$ . The following formula describes the principle

of calibration of CDOM fluorescence intensity versus that of the quinine sulphate concentration:

$$I_s = \frac{I_{\text{CDOM}}}{I_{\text{qs}}}, \quad (3)$$

where  $I_s$  is the standardized fluorescence intensity in [QSE],  $I_{\text{CDOM}}$  is the fluorescence intensity of the CDOM sample, and the  $I_{\text{qs}}$  is the fluorescence intensity of a given concentration of quinine sulphate solution.

The MicroFlu-CDOM fluorometer was calibrated in two amplification modes: high – in the 0–20 QSE range, and low – in the 0–200 QSE range. The calibration curve is stored in the instrument's EPROM microprocessor, and the fluorometer readings are transmitted by telemetry cable in digital connection mode in two formats: raw counts and calibrated QSE values. The instrument has an alternative connection mode through a standardized analogue output socket. The signal is transmitted as DC voltage within a range of 0–5 Volts. The voltage can be converted to QSE units with the following formula:

$$I_{\text{sample}} = I_{\text{qs max}} \frac{V_{\text{sample}}}{V_{\text{max}}}, \quad (4)$$

where  $I_{\text{sample}}$  [QSE] is the fluorescence intensity of the CDOM in the water sample,  $I_{\text{qs max}}$  [QSE] is the maximum fluorescence intensity of the quinine sulphate solution in a given amplification mode,  $V_{\text{sample}}$  [Volts] is the voltage reading transmitted by the fluorometer during sampling, and  $V_{\text{max}}$  [Volts] is the voltage signal when sampling the maximum quinine sulphate concentration in a given amplification mode.  $I_{\text{max}} = 20$  QSE is set up for the high amplification mode, and  $I_{\text{max}} = 200$  QSE is set up for the low amplification mode,  $V_{\text{max}} = 5$  Volts.

The CDOM fluorescence intensity measured in situ can be influenced by the presence of particles and other soluble compounds that can interfere with the excitation and emission of light on the optical path between the sample volume and the instrument optical window (Belzile et al. 2006). In order to quantify the impact of particles on the CDOM fluorescence signal measured with the TRIOS MicroFlu-CDOM fluorometer, measurements were made before and after the water samples were filtered. The MicroFlu-CDOM fluorometer was deployed (from March 2008 until April 2009) on a specially designed calibration stand. Water samples were taken from the same Niskin bottle and one portion of unprocessed water was stored in a clean glass beaker, while the second was filtered with the same method described above for the spectrophotometric scans. The portion of filtered water was then placed in another clean glass beaker. The fluorescence of the unprocessed raw water and filtered water was measured for 3 minutes in each beaker

in the calibration stand. The fluorometer was monitored with a computer via the power supply, and the telemetry monitoring unit was checked via a digital connection. The fluorescence intensities of raw and filtered water were stored in the data base for further statistical analysis.

### **2.3. In situ measurements of environmental variables, CDOM fluorescence and spectral attenuation and absorption**

During field measurements in 2008 and 2009, temperature and salinity profiles were measured at each sampling station using a SeaBird SB47 CTD probe to collect information on the hydrological state of the marine environment.

In addition to collecting water samples for spectroscopic measurements in the laboratory of the inherent optical properties of the sea water, inherent optical properties were also measured in situ using an ac-9 plus (WETLabs Inc., USA) spectral attenuation and absorption meter. In situ measurements of the light absorption  $a$  and attenuation  $c$  were performed at wavelengths of 412, 440, 488, 510, 532, 555, 650, 676 and 715 nm. The instrument was calibrated in pure water and routinely checked for stability with air-readings. Air offset, temperature and salinity corrections were applied according to the manual. Since the ac-9 absorption signal needs correction for scattering, the so-called 'Zaneveld method' was applied, which assumes zero absorption for 715 nm (Zaneveld et al. 1995).

From May 2009 onwards, the TRIOS MicroFlu-CDOM fluorometer and SeaBird SB47 CTD were coupled with the WETLabs ac-9 plus spectrophotometer, which functioned as the data integrator. The instrument setup, referred to as the Integrated Optical-Hydrological Probe, was fitted into one rig and connected by telemetry cable with the power supply and data transmission and control deck unit. The ac-9 plus and CTD water intakes were installed on the same horizontal plane as the optical window of the fluorometer. The signals from all the sensors were transmitted in real time via the telemetry cable to a laptop on board, where they were merged and synchronized along with their time stamps with WAP 4.25 software supplied by WETLabs Inc. USA. All of the signals were processed further using software written in the Matlab® environment. This had calibration procedures for all the sensors, and it merged all the measured geophysical parameters and calibrated values in physical units into a depth binned matrix. The Integrated Optical-Hydrological Probe was deployed as a profiling instrument to acquire the vertical distribution of optical parameters, salinity and temperature as functions of depth.

## 2.4. DOC concentration

Samples for DOC measurements were passed through 0.2  $\mu\text{m}$  pre-cleaned membrane filters. A total of 40 ml aliquots of filtrate were acidified with 150  $\mu\text{l}$  0.1 M HCl and stored in the dark at 5°C until laboratory analysis. These were done in a ‘HyPerTOC’ analyser (Thermo Electron Corp., The Netherlands) using UV/persulphate oxidation and non-dispersive infrared detection (Sharp 2002). Measurements of each sample using the standard addition method (potassium hydrogen phthalate) were performed in triplicate. Quality control of DOC concentrations was performed with reference material supplied by Hansell Laboratory, University of Miami. The methodology ensured satisfactory accuracy (average recovery 95%;  $n = 5$ ; CRM = 44 – 46  $\mu\text{M C}$ ; our results = 42 – 43  $\mu\text{M C}$ ) and precision characterized by a relative standard deviation (RSD) of 2%.

The carbon-specific CDOM absorption coefficients at two wavelengths – 350 nm,  $a^*_{\text{CDOM}}(350)$ , and 370 nm,  $a^*_{\text{CDOM}}(370)$  – were calculated as the ratio of the CDOM absorption coefficient at a given wavelength  $a_{\text{CDOM}}(\lambda)$  to the DOC concentration (eq. (5)). The carbon-specific fluorescence intensity was defined in the same way as the carbon-specific CDOM absorption coefficient: the total fluorescence intensity was normalized by the DOC concentration:

$$a^*_{\text{CDOM}}(\lambda) = \frac{a_{\text{CDOM}}(\lambda)}{\text{DOC}}. \quad (5)$$

## 3. Results

### 3.1. Seasonal variability of CDOM optical properties and concentration of Dissolved Organic Carbon

The CDOM absorption coefficient at 370 nm  $a_{\text{CDOM}}(370)$  was chosen to describe changes in CDOM quantity. This wavelength is the maximum of the excitation band of the in situ CDOM fluorometer. The CDOM absorption spectrum slope coefficient  $S$  was used to differentiate CDOM pools. To assess the seasonal dynamics of CDOM optical properties and to compare the present results with published data records on CDOM in the Baltic Sea, this data set was split according to the criteria used by Kowalczyk (1999).

The detailed descriptive statistics of the  $a_{\text{CDOM}}(370)$ ,  $S$  and CDOM fluorescence intensity in raw and filtered water and DOC concentration are presented in Table 2. The temporal and spatial changes of CDOM optical properties followed the well-established seasonal pattern described in previous papers (e.g. Kowalczyk 1999, Kowalczyk et al. 2005). The lowest mean value of  $a_{\text{CDOM}}(370)$  was recorded in autumn–winter

**Table 2.** Seasonal mean values for  $a_{\text{CDOM}(370)}$ ,  $S$ , and CDOM fluorescence intensities in raw and filtered water, carbon-specific CDOM absorption coefficient,  $a^*_{\text{CDOM}(370)}$ 

Parameter	$a_{\text{CDOM}(370)}$ [ $\text{m}^{-1}$ ]	$S$ [ $\text{nm}^{-1}$ ]	$I_{\text{F1}} - \text{raw water}$ [QSE]	$I_{\text{F1}} - \text{filtered water}$ [QSE]	DOC [ $\mu\text{M C}$ ]	$a^*_{\text{CDOM}(370)}$ [ $\text{mM C}^{-1} \text{m}^2$ ]
spring						
mean	1.82	0.0196	25.31	27.77	397.6	0.00428
SD	1.35	0.003	18.12	20.18	94.7	0.00183
variability range	0.70–7.94	0.0120–0.0303	5.03–84.95	4.86–113.7	288.5–831.7	0.00215–0.0116
$n$	250	250	107	106	242	234
summer						
mean	1.78	0.0160	23.66	29.73	359.2	0.00469
SD	1.06	0.002	69.63	18.74	47.4	0.00178
variability range	1.06–6.54	0.0127–0.0210	11.66–69.63	9.86–8097	303.7–559.2	0.00301–0.0115
$n$	86	86	82	28	84	82
autumn–winter						
mean	1.57	0.0174	22.80	24.06	346.5	0.00442
SD	0.96	0.002	21.44	24.86	59.8	0.00132
variability range	0.93–5.56	0.0125–0.0226	3.27–116.11	3.88–122.97	266.7–583.3	0.00258–0.0101
$n$	140	140	136	114	139	140
all data						
mean	1.76	0.01830	23.84	26.29	375.4	0.00438
SD	1.20	0.00275	18.50	22.33	81.7	0.00175
variability range	0.70–7.94	0.0120–0.0303	3.27–116.11	3.88–122.97	266.7–831.7	0.00215–0.0116
$n$	476	476	325	248	465	456

(average  $a_{\text{CDOM}}(370) = 1.57 \text{ m}^{-1}$ ), the highest mean value of  $a_{\text{CDOM}}(370)$  in spring (average  $a_{\text{CDOM}}(370) = 1.82 \text{ m}^{-1}$ ). The range of variability of the CDOM absorption coefficient  $a_{\text{CDOM}}(370)$  in the data set selected for this study was  $0.70 - 7.94 \text{ m}^{-1}$ , which was within the published range of the variability of the CDOM absorption coefficient in the Baltic Sea, after the appropriate spectral adjustments had been made (Kowalczyk 1999, Kowalczyk et al. 2005, 2006). The fluorescence intensity measured in both the raw and filtered water, and also the DOC concentration, followed the same temporal trend: increasing intensity and concentration in spring and a gradual decrease with the approach of the cold season. The temporal variations in the spectral slope coefficient  $S$  were different in the present study. The minimum of the average value of this coefficient was observed in the summer. The seasonal distribution of the carbon-specific CDOM absorption coefficient  $a^*_{\text{CDOM}}(370)$  was similar in all the seasons considered, and the average values of this parameter were almost invariant. This is easily explained by the seasonal distributions of  $a_{\text{CDOM}}(370)$  and DOC, which have the same seasonal cycles. Both parameters had the highest values in spring, thereafter decreasing steadily towards the cold season; their ratio thus remained stable.

On the basis of the results of the simple descriptive statistics, it can be concluded that this relatively small data set provides a good representation of the variations in CDOM optical properties in the study area, and can be regarded as statistically representative.

### **3.2. Relationships between CDOM absorption coefficient, CDOM fluorescence and Dissolved Organic Carbon concentration**

In order to quantify the impact of particles on DOM-FL measured with the TRIOS MicroFlu-CDOM fluorometer, fluorescence intensities measured in filtered water vs. those measured in raw water were compared; 245 data pairs were recorded for both quantities. A thorough error assessment was performed by calculating the Bias, defined as the average difference between the fluorescence intensity measured in raw and filtered water, and the RMSE of the absolute difference (AD) and the relative percent difference (RPD) between fluorescence intensities measured in raw and filtered water. The relative percentage difference was defined as the ratio of the absolute difference to the fluorescence intensity measured in the filtered water multiplied by 100%. The value of the Bias calculated for AD was  $-1.67 \text{ QSE}$ , and the RSME for the same parameter was  $6.37 \text{ QSE}$ . The Bias, which is a measure of systematic error, indicated that the presence of particles in the raw water would decrease the fluorescence

intensity compared to the fluorescence intensities in the filtered water. The values of the Bias and the RSME calculated for RPD were  $-2.05\%$  and  $34.31\%$  respectively. The Bias calculated for the absolute difference is low compared to the average fluorescence intensities of raw and filtered water, but the effect of particle presence could vary significantly, since, when the relative percentage difference was considered, it could be as high as  $35\%$ . The presence of particles would significantly reduce the performance of the in situ deployment of the MicroFlu-CDOM fluorometer in turbid water with low contents of dissolved organic material.

Regression analysis between the fluorescence intensities measured in the raw and filtered water was also performed to check the consistency of data distribution in both data sets. Figure 2a presents the distribution of the  $I_{F1}$  measured in the raw water vs.  $I_{F1}$  measured in the filtered water. The fluorescence intensity measured in the raw water follows the same trend linearly as that measured in the filtered water. The results of regression analysis are described by the equation

$$I_{F1\_raw} = 0.878 \pm 0.011 \times I_{F1\_filtered} + 1.266 \pm 0.413. \quad (6)$$

The Pearson correlation coefficient was  $R^2 = 0.98$  and the determination coefficient was  $R^2 = 0.97$ ; both slope coefficient and intercept were statistically significant at the  $I_{F1\_filtered}$  confidence level of  $p < 0.01$ , sample size

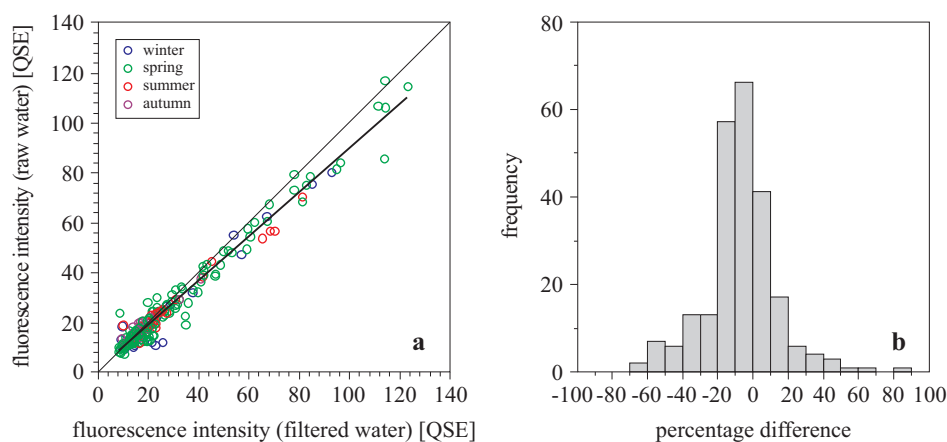


**Figure 2.** a) Distribution of the fluorescence intensity measured in raw water  $I_{F1\_raw}$  using the TRIOS MicroFlu-CDOM fluorometer as a function of the fluorescence intensity measured in filtered water  $I_{F1\_filtered}$ . The thin solid line represents the 1:1 line between the two parameters, the thick solid line represents the regression line between the two parameters. Samples collected in different seasons are marked in colours; b) Histogram of relative percentage differences between fluorescence intensities measured in raw and filtered water

$n = 210$ . The positive intercept of the regression equation can be interpreted as the fluorescence signal due to the organic coating of particles caused by DOM adsorption on particles (Shank et al. 2005) or the fluorescence signal due to the fluorescent organic matter contained in organic particles. The absolute difference between  $I_{F1\_raw}$  and  $I_{F1\_filtered}$  increases with the increased fluorescence level caused by higher concentrations of optically-active DOM. The primary source of DOM in the Baltic Sea is riverine input, so elevated values of both  $I_{F1\_raw}$  and  $I_{F1\_filtered}$  are usually recorded in areas influenced by freshwater inflows into the Baltic Sea. In the vicinity of river mouths turbidity is usually higher, as expressed by elevated values of the absorption and the beam attenuation coefficients measured by the ac-9 meter. Elevated spectral values of the beam attenuation coefficient are an indicator of high concentrations of suspended particles. Thus, higher concentrations of particles resulted in a higher absolute difference between  $I_{F1\_raw}$  and  $I_{F1\_filtered}$ . Figure 2b presents a histogram of the distribution of the relative percentage difference of RPD between  $I_{F1\_raw}$  and  $I_{F1\_filtered}$ . The statistical distribution of RPD was almost normal with a single maximum centred around the  $\pm 10\%$  difference. The tail of positive values of RPD indicated that, in some cases,  $I_{F1\_raw}$  could have higher values than  $I_{F1\_filtered}$ . This situation is usually noted in the open waters of the Baltic Sea, which are outside the direct influence of freshwater discharge, and where concentrations of DOM are lower. At a low DOM fluorescence intensity of around 10 QSE,  $I_{F1\_raw}$  was higher than  $I_{F1\_filtered}$ . This can be explained by the compensation for the loss of the DOM fluorescence signal

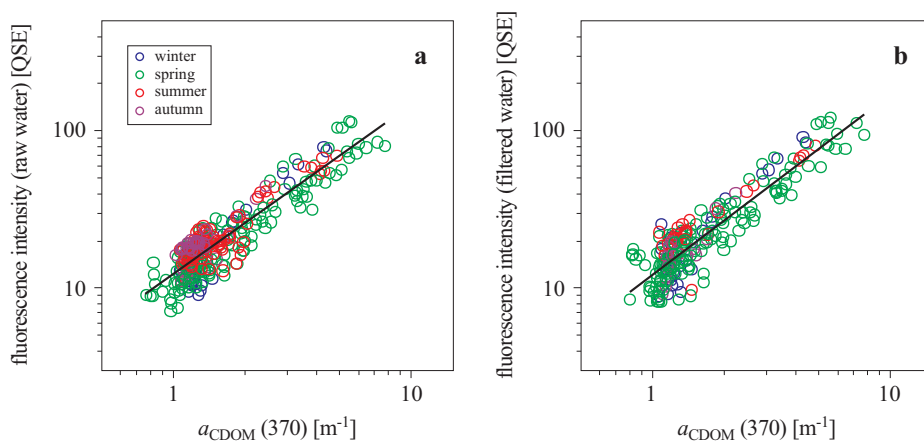


**Figure 3.** Relationship between the CDOM absorption coefficient  $a_{CDOM}(370)$  and the DOM fluorescence intensity measured in raw water  $I_{F1\_raw}$  (a) and the DOM fluorescence intensity measured in filtered water  $I_{F1\_filtered}$  (b). Samples collected in different seasons are marked in colours



**Table 3.** Results of regression analysis between the CDOM absorption coefficient fluorescence intensity measured in raw and filtered waters, and DOC concentrations

Parameters	Regression coefficients		R	R <sup>2</sup>	Sample size
	Slope <i>a</i>	Intercept <i>b</i>			
<i>a</i> <sub>CDOM(370)</sub> vs. <i>I</i> <sub>F1_raw</sub>					
all data	14.602 ± 0.358	-2.146 ± 0.779	0.92	0.85	297
spring	14.347 ± 0.515	-2.939 ± 1.304	0.92	0.84	145
summer	14.875 ± 0.563	-1.578 ± 1.061	0.95	0.90	79
autumn-winter	19.344 ± 1.216	-6.815 ± 1.943	0.88	0.78	71
<i>a</i> <sub>CDOM(370)</sub> vs. <i>I</i> <sub>F1_filtered</sub>					
all data	16.758 ± 0.424	-4.549 ± 0.969	0.93	0.87	226
spring	16.291 ± 0.512	-4.666 ± 1.260	0.93	0.87	149
summer	16.569 ± 0.656	-0.755 ± 1.410	0.98	0.96	26
autumn-winter	23.928 ± 0.917	-15.049 ± 1.573	0.96	0.93	49
DOC vs. <i>a</i> <sub>CDOM(370)</sub>					
all data	0.0123 ± 0.0003	-2.887 ± 0.124	0.87	0.76	459
spring	0.0130 ± 0.0003	-3.281 ± 0.137	0.91	0.83	299
summer	0.0079 ± 0.0007	-0.902 ± 0.226	0.71	0.50	116
autumn-winter	0.0119 ± 0.0013	-2.408 ± 0.411	0.74	0.54	75
DOC vs. <i>I</i> <sub>F1_raw</sub>					
all data	0.179 ± 0.009	-42.631 ± 3.547	0.75	0.56	291
spring	0.202 ± 0.012	-56.018 ± 5.215	0.81	0.65	142
summer	0.198 ± 0.023	-47.190 ± 8.628	0.68	0.49	78
autumn-winter	0.225 ± 0.035	-51.463 ± 11.337	0.61	0.37	71
DOC vs. <i>I</i> <sub>F1_filtered</sub>					
all data	0.209 ± 0.0114	-53.260 ± 4.468	0.78	0.61	222
spring	0.224 ± 0.013	-63.059 ± 5.462	0.82	0.67	145
summer	0.285 ± 0.027	-75.073 ± 9.891	0.90	0.81	26
autumn-winter	0.316 ± 0.040	-81.513 ± 13.065	0.75	0.56	49

All variables were fitted to the linear equation  $y = a \times x + b$ , where  $x = a_{\text{CDOM}(370)}$  or  $x = \text{DOC}$  respectively. Regression coefficients, Pearson's correlation coefficient R and coefficient of determination R<sup>2</sup> are significant at a confidence level of  $p < 0.01$ .

because of the presence of suspended particles, by the residual fluorescence of the DOM adsorbed on particle surfaces, or by the fluorescence of organic matter contained in the tissues of organic particles.

There was a strong linear relationship between fluorescence intensity and the CDOM absorption coefficient at the excitation wavelength  $a_{\text{CDOM}(370)}$ . Figure 3 shows the distribution of  $I_{\text{F1\_raw}}$  (Figure 3a) and  $I_{\text{F1\_filtered}}$  (Figure 3b) as a function of  $a_{\text{CDOM}(370)}$ . The empirical relationship between  $a_{\text{CDOM}(370)}$  and  $I_{\text{F1\_filtered}}$  was better than the analogous empirical relationship between  $a_{\text{CDOM}(370)}$  and  $I_{\text{F1\_raw}}$ . The possible influence of particles suspended in raw water could have diminished the values of the

correlation coefficient and coefficient of determination calculated for the  $a_{\text{CDOM}}(370)$  and  $I_{\text{Fl\_raw}}$  relationship. Seasonal variability of the CDOM optical properties of  $a_{\text{CDOM}}(370)$ ,  $I_{\text{Fl\_raw}}$  and  $I_{\text{Fl\_filtered}}$  influenced the results of the regression analysis of the statistical relationships between these parameters. Table 3 contains detailed results of the analysis of the linear regression between CDOM optical properties and DOC concentration that accounts for seasonal cycles. The population data analysed was dominated by samples collected in spring; therefore, the regression coefficients calculated for the spring data set are closest to those calculated for the whole data set. The slope coefficients in the relationships between  $a_{\text{CDOM}}(370)$ ,  $I_{\text{Fl\_raw}}$  and  $I_{\text{Fl\_filtered}}$  were very similar in spring and summer; however, there were statistically significant differences in the intercept values caused by the smaller variability range of CDOM optical properties in summer as compared to those in spring. The differences in the values of Pearson's correlation coefficient and the determination coefficient between seasons could stem from different sample sizes in the data subsets. The set of coefficients that determines the empirical relationships between  $a_{\text{CDOM}}(370)$ ,  $I_{\text{Fl\_raw}}$  and  $I_{\text{Fl\_filtered}}$  calculated for the autumn-winter data subset differed significantly from that presented above. The linear relationship between these parameters was characterized by significantly higher slope and intercept coefficients. Overall, high values of Pearson's correlation coefficient  $R$  and a high determination coefficient  $R^2$  in the results presented suggest that fluorescence can be regarded as a proxy for the absorption coefficient in Baltic Sea waters, but seasonal variability should also be considered.

The linear relationships between DOC concentration and the CDOM optical properties of  $a_{\text{CDOM}}(370)$ ,  $I_{\text{Fl\_raw}}$  and  $I_{\text{Fl\_filtered}}$  are presented in Figures 4 and 5. The relationship between DOC and  $a_{\text{CDOM}}(370)$  had a higher Pearson's correlation coefficient and determination coefficient than did the linear relationship between fluorescence intensities measured in raw and filtered water. Like the relationships between  $a_{\text{CDOM}}(370)$ ,  $I_{\text{Fl\_raw}}$  and  $I_{\text{Fl\_filtered}}$ , the relationship between DOC concentration and the fluorescence intensity measured in the filtered sea water was much better than the analogous empirical relationship between DOC concentration and fluorescence intensity measured in the unprocessed sea water.

Based on the regression coefficient presented in Table 3, the optically inactive fraction of DOC was calculated by extrapolating the regression equation to 0 values of CDOM absorption and the respective fluorescence intensities. The standard error of estimation for the respective linear regression equations was used to calculate the confidence intervals. Values of the optically inactive DOC fraction (with confidence intervals) were very

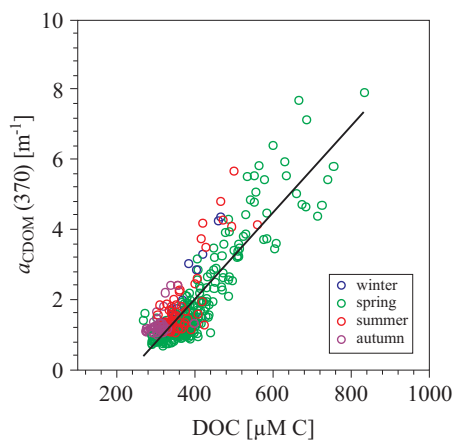


**Figure 4.** Relationship between the concentration of Dissolved Organic Carbon and the CDOM absorption coefficient  $a_{\text{CDOM}(370)}$ . Samples collected in different seasons are marked in colours

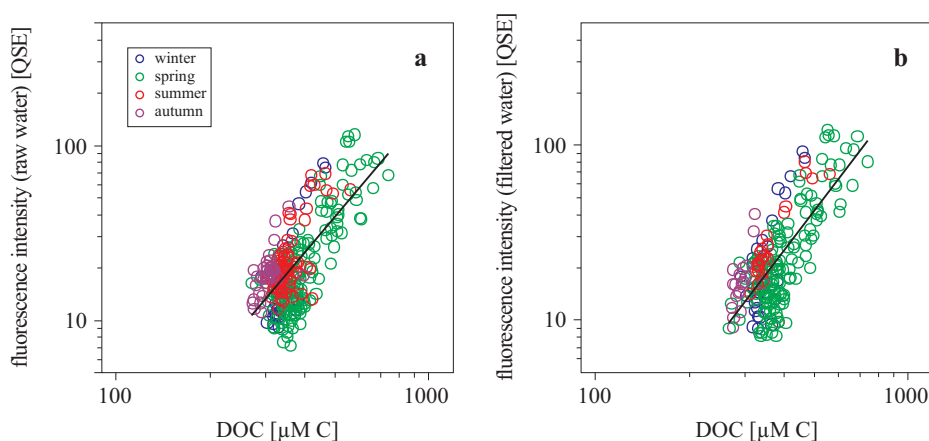


**Figure 5.** Relationship between the concentration of Dissolved Organic Carbon and DOM fluorescence intensity measured in raw water  $I_{\text{F1}_{\text{raw}}}$  (a) and DOM fluorescence intensity measured in filtered water  $I_{\text{F1}_{\text{filtered}}}$  (b). Samples collected in different seasons are marked in colours

similar in the relationships between DOC and  $a_{\text{CDOM}(370)}$ ,  $I_{\text{F1}_{\text{raw}}}$  and  $I_{\text{F1}_{\text{filtered}}}$  estimated for the complete data set (see Table 4 for details). The non-absorbing DOC fraction was  $234.72 \pm 15.82 \mu\text{M C}$ . The non-fluorescing DOC fraction was estimated at  $238.16 \pm 31.87 \mu\text{M C}$  for fluorescence measured in raw water and  $254.83 \pm 34.89 \mu\text{M C}$  for that measured in filtered water. The confidence intervals of estimation of the optically inactive DOC fraction for the respective regression equations

**Table 4.** Values of the optically inactive DOC fraction calculated from respective relationships between  $a_{\text{CDOM}}(370)$ ,  $I_{\text{F1\_raw}}$ ,  $I_{\text{F1\_filtered}}$  and DOC concentration in seasons

	Optically inactive DOC fraction [ $\mu\text{M C}$ ]	Confidence intervals
DOC vs. $a_{\text{CDOM}}(370)$		
all data	234.72	$\pm 15.82$
spring	252.39	$\pm 16.37$
summer	114.18	$\pm 39.03$
autumn–winter	202.35	$\pm 57.33$
DOC vs. $I_{\text{F1\_raw}}$		
all data	238.16	$\pm 31.87$
spring	277.32	$\pm 42.44$
summer	238.33	$\pm 72.24$
autumn–winter	228.72	$\pm 88.10$
DOC vs. $I_{\text{F1\_filtered}}$		
all data	254.83	$\pm 34.89$
spring	281.51	$\pm 40.86$
summer	263.41	$\pm 60.20$
autumn–winter	257.95	$\pm 75.20$

overlap; this suggests that differences in estimating the non-absorbing and non-fluorescent DOC fractions are statistically insignificant. Therefore, fluorescence measured in situ could be regarded as an approximate proxy for DOC concentration. The concentrations of the optically inactive fractions of DOC calculated for the respective regression equations in the seasons were highest in spring and lowest in summer with intermediate values in autumn–winter. However, the seasonal confidence intervals of these estimates also increased; therefore the observed trend cannot be regarded as statistically significant. The only exception was the non-absorbing DOC fraction calculated for the summer relationship between DOC and  $a_{\text{CDOM}}(370)$ . The proportion of the optically inactive DOC fraction in the Baltic Sea is very high. The average proportion of the optically inactive DOC fraction in the Baltic Sea calculated for the whole data set was 62.5%. The proportion of the optically inactive DOC fraction changes from season to season: it was 63.5% in spring, 31.8% in summer and 58.4% in autumn–winter.

### 3.3. Relationships between carbon-specific CDOM absorption and carbon-specific fluorescence with $a_{\text{CDOM}}(370)$ fluorescence intensity

The values of the organic carbon-specific CDOM absorption coefficient  $a^*_{\text{CDOM}}(370)$  ranged within one order of magnitude from 0.0044

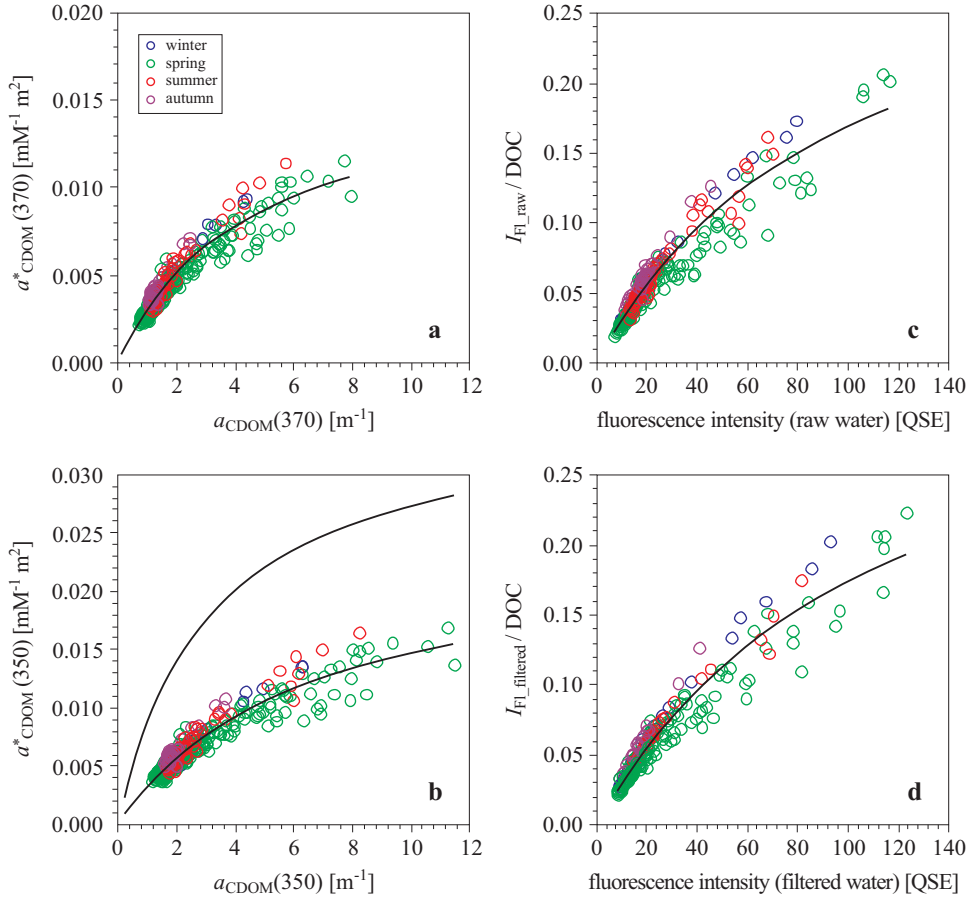


**Figure 6.** Relationship between the CDOM absorption coefficient  $a_{\text{CDOM}}(370)$  vs. the carbon-specific CDOM absorption coefficient  $a^*_{\text{CDOM}}(370)$  (a); CDOM absorption coefficient  $a_{\text{CDOM}}(350)$  vs. carbon-specific CDOM absorption coefficient  $a^*_{\text{CDOM}}(350)$  (b); DOM fluorescence intensity measured in raw water  $I_{\text{F1\_raw}}$  vs. carbon-specific DOM fluorescence intensity measured in raw water  $I_{\text{F1\_raw}}/\text{DOC}$  (c) and DOM fluorescence intensity measured in filtered water  $I_{\text{F1\_filtered}}$  vs. carbon-specific DOM fluorescence intensity measured in filtered water  $I_{\text{F1\_filtered}}/\text{DOC}$  (d). The thick solid line on panel (b) represents the non-linear regression between  $a_{\text{CDOM}}(350)$  vs. carbon-specific CDOM absorption coefficient  $a^*_{\text{CDOM}}(350)$ , estimated in Atlantic coastal waters off the eastern coast of the USA by Kowalczyk et al. (2010). The thin solid line represents the non-linear regression between  $a_{\text{CDOM}}(350)$  vs. carbon-specific CDOM absorption coefficient  $a^*_{\text{CDOM}}(350)$ , estimated in the Baltic Sea in the current study. Samples collected in different seasons are marked in colours

to  $0.0116 \text{ mM}^{-1} \text{ m}^2$ . The highest values of  $a^*_{\text{CDOM}}(370)$  were observed in the Gulf of Gdańsk and the Pomeranian Bay in close proximity to

**Table 5.** Results of regression analysis between CDOM absorption coefficient and carbon-specific CDOM absorption coefficient, fluorescence intensity measured in raw and filtered water vs. respective carbon-specific fluorescence intensity and salinity vs. CDOM optical properties and DOC concentrations

Parameters	Equation type	Regression coefficients	R	R <sup>2</sup>	Sample size
$a_{\text{CDOM}(370)}$ vs. $a^*_{\text{CDOM}(370)}$	hyperbolic $y = a \times x / (b + x)$	$a = 0.0166 \pm 0.0004$ $b = 4.4199 \pm 0.1641$	0.96	0.91	458
$a_{\text{CDOM}(350)}$ vs. $a^*_{\text{CDOM}(350)}$	hyperbolic $y = a \times x / (b + x)$	$a = 0.0239 \pm 0.0006$ $b = 6.2817 \pm 0.2321$	0.95	0.91	458
$I_{\text{Fl}_{\text{raw}}}$ vs. $I_{\text{Fl}_{\text{raw}}}/\text{DOC}$	hyperbolic $y = a \times x / (b + x)$	$a = 0.3416 \pm 0.0157$ $b = 102.146 \pm 6.494$	0.96	0.91	290
$I_{\text{Fl}_{\text{filtered}}}$ vs. $I_{\text{Fl}_{\text{filtered}}}/\text{DOC}$	hyperbolic $y = a \times x / (b + x)$	$a = 0.3778 \pm 0.0191$ $b = 117.222 \pm 8.327$	0.96	0.93	221
salinity vs. $a_{\text{CDOM}(370)}$	linear $y = a \times x + b$	$a = -0.687 \pm 0.014$ $b = 6.164 \pm 0.094$	-0.89	0.80	476
salinity vs. $I_{\text{Fl}_{\text{raw}}}$	linear $y = a \times x + b$	$a = -11.459 \pm 0.236$ $b = 100.015 \pm 1.605$	-0.95	0.90	270
salinity vs. $I_{\text{Fl}_{\text{filtered}}}$	linear $y = a \times x + b$	$a = -12.903 \pm 0.292$ $b = 111.118 \pm 1.967$	-0.95	0.91	195
salinity vs. DOC	linear $y = a \times x + b$	$a = -38.092 \pm 1.493$ $b = 621.360 \pm 10.186$	-0.78	0.61	418

All variables were fitted to the equation type in the second column. All regression coefficients and coefficients of determination are significant at a confidence level of  $p < 0.01$ .

the Vistula and Odra river mouths in spring. The lowest values of  $a^*_{\text{CDOM}(370)}$  were recorded in the open waters of the Baltic Sea, also in spring. The spatial distribution of organic carbon-specific CDOM absorption coefficients observed in this region (decrease of carbon-specific CDOM absorption coefficient with increasing distance from terrestrial sources) agreed well with observations from other regions (e.g. Rochelle-Newall & Fisher 2002a, Del Vecchio & Blough 2004, Kowalczyk et al. 2010). Values of  $a^*_{\text{CDOM}(370)}$  were plotted as a function of the CDOM absorption coefficient  $a_{\text{CDOM}(370)}$  (Figure 6a). To compare the present results with those of other studies, values of  $a^*_{\text{CDOM}(350)}$  were plotted as a function of  $a_{\text{CDOM}(350)}$  (Figure 6b). Similarly, carbon-specific fluorescence intensities were plotted against the fluorescence intensity measured in raw and filtered water (Figure 6c,d). The distribution of  $a^*_{\text{CDOM}(370)}$  as a function of  $a_{\text{CDOM}(370)}$  and the distribution of  $I_{\text{Fl}_{\text{raw}}}/\text{DOC}$  and  $I_{\text{Fl}_{\text{filtered}}}/\text{DOC}$  as functions of the respective fluorescence intensities were very similar. These distributions were approximated using a hyperbolic function – the

approximation was a very good one, as indicated by the high values of the coefficient of determination at  $R^2 = 0.91$  for all the presented relationships:  $a_{\text{CDOM}(370)}$  vs.  $a^*_{\text{CDOM}(370)}$ ,  $a_{\text{CDOM}(350)}$  vs.  $a^*_{\text{CDOM}(350)}$ ,  $I_{\text{Fl\_raw}}$  vs.  $I_{\text{Fl\_raw}}/\text{DOC}$  and  $I_{\text{Fl\_filtered}}$  vs.  $I_{\text{Fl\_filtered}}/\text{DOC}$  (see Table 5 for detailed results of the regression analysis). The hyperbolic function distributions suggest there is an asymptotic relationship between these parameters.

### 3.4. Relationships between CDOM optical properties and salinity

Previous studies of the distribution of CDOM optical properties in the Baltic Sea indicate that the CDOM absorption coefficient and fluorescence intensities are inversely correlated with salinity (Højerslev 1988, 1989, Kowalczyk & Kaczmarek 1996, Ferrari & Dowell 1998, Kowalczyk 1999). The negative trends of CDOM optical properties and DOC concentration are presented in Figures 7. All of the relationships examined between CDOM optical properties and DOC concentration vs. salinity were statistically significant and had very high correlation coefficients (Table 5). The fluorescence intensity measured in both raw and filtered water was best correlated with salinity (inverse relationship); Pearson's correlation coefficient was  $R = -0.95$  in both cases. The mixing of fresh and saline waters alone could explain up to 90% of the variability of the fluorescence intensity. The CDOM absorption coefficient  $a_{\text{CDOM}(370)}$  is also inversely correlated with salinity:  $R = -0.89$ ,  $R^2 = 80$ . The lower values of the correlation and determination coefficients could be the result of the much larger sample size used for the regression analysis. The linear relationship between salinity vs. DOC is statistically significant, although the correlation and determination coefficients calculated were the smallest in all of the relationships analysed. The input of DOC from terrigenous sources and its mixing with marine waters is the primary driver of DOC variability in the southern Baltic Sea. These processes could be responsible for 60% of the DOC variability in the marine environment, but there are certainly other non-linear processes that need to be included in the organic carbon budget, like the autochthonous production of DOC in the primary production process and the bacterial and photochemical mineralization of DOC. The intercept of the relationships of CDOM optical properties and DOC concentration vs. salinity could be regarded as a value characteristic of the terrestrial end member. The value of  $a_{\text{CDOM}(370)}$  that could characterize fresh water is  $6.62 \text{ m}^{-1}$ , and the respective values of the fluorescence intensities are  $I_{\text{Fl\_raw}} = 100.02 \text{ QSE}$  and  $I_{\text{Fl\_filtered}} = 111.12 \text{ QSE}$ . The average DOC concentration characteristic of fresh waters is  $621.36 \mu\text{M C}$ . There were some outliers from the general trend

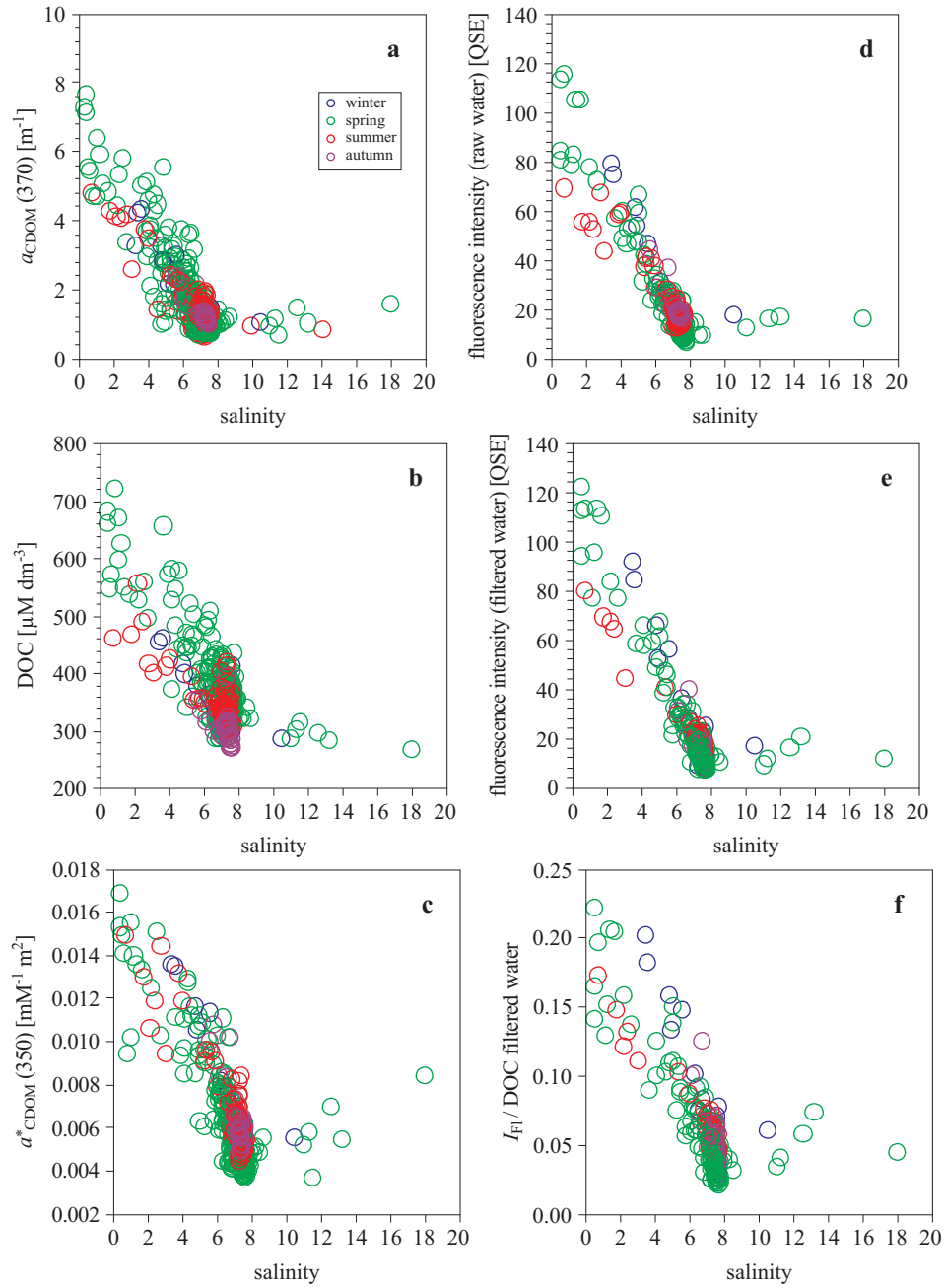


**Figure 7.** Distribution of the CDOM absorption coefficient  $a_{\text{CDOM}}(370)$  (a), concentration of Dissolved Organic Carbon (b)  $a^*_{\text{CDOM}}(370)$  (c), DOM fluorescence intensity measured in raw water  $I_{\text{Fl}_{\text{raw}}}$  (d), DOM fluorescence intensity measured in filtered water  $I_{\text{Fl}_{\text{filtered}}}$  (e) and carbon specific DOM fluorescence intensity measured in filtered water  $I_{\text{Fl}_{\text{filtered}}}/\text{DOC}$  (f) as a function of salinity. Samples collected in different seasons are marked in colours



(see Figure 7). Samples identified as outliers were examined thoroughly in terms of date, time, geographic location of sampling station and depth, and the prevailing hydrographic conditions at the sites where these samples were collected. All of these samples were collected in the Baltic Sea deeps of Bornholm, Gdańsk and Gotland at depths greater than 60 m below the permanent pycnocline separating the surface layer of low saline water that undergoes seasonal stratification and deep mixing from the stagnant deep waters that originate from the North Sea and are transported through the Danish Straits during episodic inflow events. Continuous depth profiles of CDOM fluorescence carried out using the Integrated Optical-Hydrological Probe during two cruises in September and October 2009 were very useful for verifying this unusual distribution of CDOM optical properties with salinity. Two distinct distributions of fluorescence intensities as functions of depth, measured during a single field survey in September 2009, were selected. The depth profiles of the salinity and temperature are presented in Figure 8 (Figure 8a, yellow and green lines respectively) together with fluorescence intensity and the total absorption coefficient of seawater minus that due to water  $a - a_w(412)$  (Figure 8b, blue and

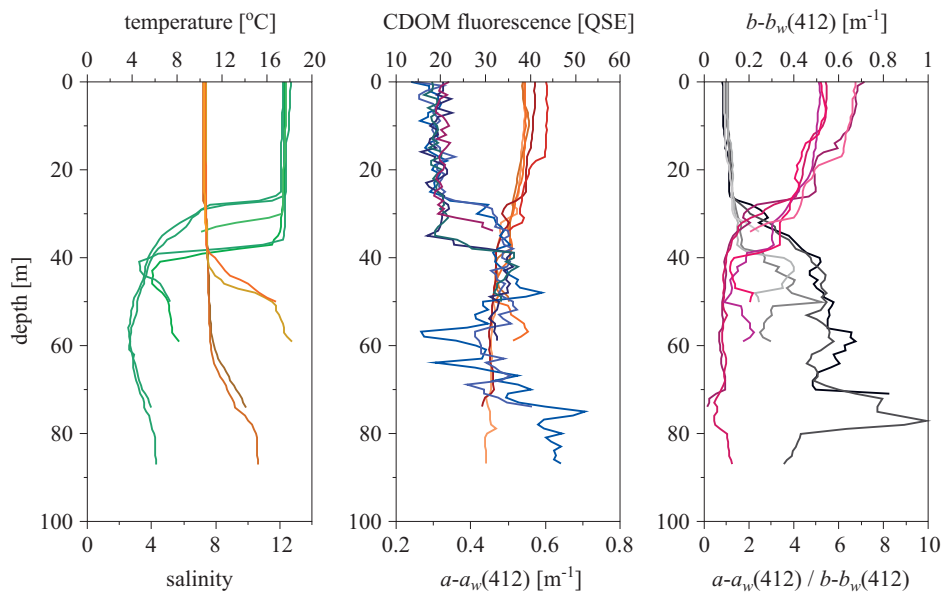


**Figure 8.** High resolution depth profiles of salinity (yellow lines), temperature (green lines), absorption coefficient less that due to water  $a - a_w(412)$  (red lines), fluorescence intensity (blue lines), scattering coefficient less that due to water  $b - b_w(412)$  (grey lines), and the ratio between absorption and scattering coefficients  $a - a_w(412) / b - b_w(412)$  (purple lines) acquired using the Integrated Optical-Hydrological Probe at deep water stations in open Baltic Sea waters

red lines respectively), the total scattering coefficient of seawater minus that due to water  $b - b_w(412)$ , and the ratio between the absorption and scattering coefficients  $a - a_w(412)/b - b_w(412)$  (Figure 8c, grey and purple lines respectively). These profiles were recorded in open Baltic Sea waters at deep water stations at the end of the summer thermal stratification period when the thermocline is at its strongest and deepest. The temperature and salinity profiles revealed three layers of water stratification: the mixed surface layer above the seasonal thermocline situated at an approximate depth of 40 m had temperatures above 16°C and a salinity of about 7.5; the deep cold water below the seasonal thermocline had temperatures of about 4°C and a salinity of about 7.5; the bottom water below the permanent pycnocline had temperatures ranging from 4 – 6°C and salinities between 8 and 12. The fluorescence profiles were almost the same for all examples presented: there was a decrease in fluorescence intensity in the mixed layer above the seasonal thermocline in comparison to the deep cold water below it, and there was a steady increase of fluorescence intensity with increasing depth below the permanent pycnocline. The absorption coefficient profiles were different from those of the fluorescence intensity. Absorption coefficient  $a - a_w(412)$  values were elevated in the mixed layer above the seasonal thermocline, but they decreased steadily with increasing depths. The differences between the depth profiles of these two variables is explained by the recorded scattering coefficient  $b - b_w(412)$ , and the ratio between absorption and scattering coefficients  $a - a_w(412)/b - b_w(412)$ . The depth profiles of the scattering coefficient in the open waters of the Baltic Sea exhibited elevated values in the mixed surface layer above the seasonal thermocline, indicating high concentrations of particles. Below the seasonal thermocline, values of  $b - b_w(412)$  decreased sharply. The depth distribution of the  $a - a_w(412)/b - b_w(412)$  ratio exhibited the lowest values in the mixed layer with monotonic increases towards the bottom. Therefore, it may be inferred that the variable contributions of absorbing particles, mainly of organic origin, to the absorption budget were responsible for the discrepancy between the depth distribution of  $I_{F1\_raw}$  and  $a - a_w(412)$ . The accumulation of particles above the seasonal thermocline during the algal growing period caused increases in the absorption coefficient. The absorption of light by CDOM decreased steadily because of its degradation in photochemical reactions and bacterial uptake (Vodacek et al. 1997). Therefore, the production and accumulation of particles compensated for the loss of absorption by CDOM in the mixed layer. Below the mixed layer the contribution of particles was much smaller and decreasing, as indicated by falls in  $b - b_w(412)$  and rises in the  $a - a_w(412)/b - b_w(412)$

ratio. Absorption was thus dominated by soluble compounds below the seasonal thermocline and the permanent pycnocline.

Another pattern for the vertical distribution of CDOM fluorescence, absorption  $a - a_w(412)$  coefficient, and scattering coefficient  $b - b_w(412)$  is presented in Figure 9. This figure illustrates the vertical distribution of the same geophysical variables with the same colour coding for them. These are the same variables as in those presented in Figure 8, but measured at sampling stations in the Gulf of Gdańsk influenced by the fresh water plume from the River Vistula. The vertical profiles of the optical parameters closely follow the thermohaline structure of the water masses. The values of all the optical parameters were elevated in the shallow lenses of plume-influenced waters in which the salinity was below 6.8. The highest values of the optical parameters were measured in the least saline water, in which the salinity was around 4.5; these decreased with increasing salinity. Below the fresh water lenses, the absorption  $a - a_w(412)$  and scattering  $b - b_w(412)$  coefficients were approximately 20% higher than those measured in the mixed layer at stations in open Baltic Sea waters. The depth profiles of

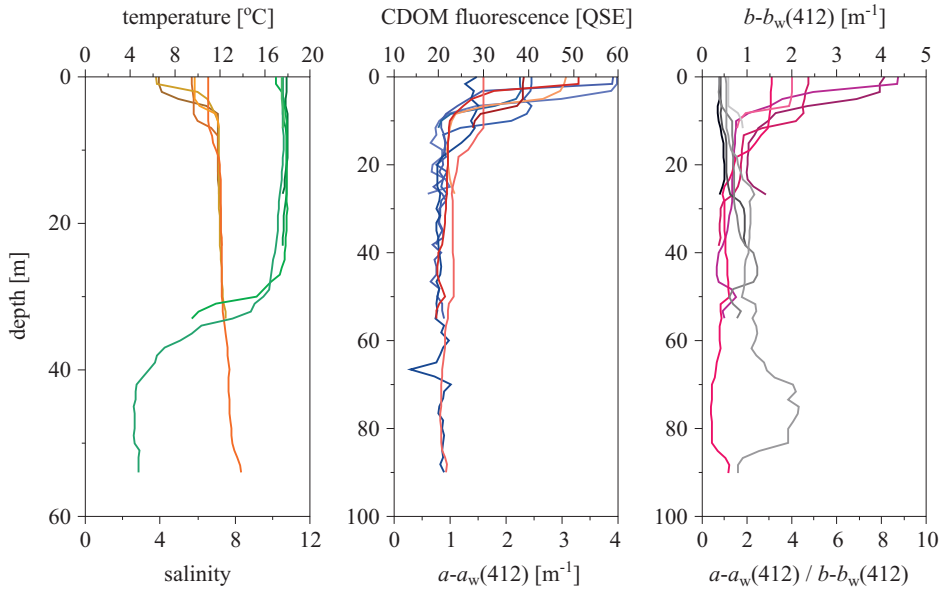


**Figure 9.** High resolution depth profiles of salinity (yellow lines), temperature (green lines), absorption coefficient less that due to water  $a - a_w(412)$  (red lines), fluorescence intensity (blue lines), scattering coefficient less that due to water  $b - b_w(412)$  (grey lines), and the ratio between absorption and scattering coefficients  $a - a_w(412) / b - b_w(412)$  (purple lines) acquired using the Integrated Optical-Hydrological Probe in the Gulf of Gdańsk at stations influenced by the Vistula river plume

CDOM fluorescence intensity below the plume-influenced water lenses were uniform throughout the depth range with values of approximately 20 QSE, which were similar to those measured in the mixed layer at the stations in the open waters of the Baltic Sea. These did not increase below the seasonal thermocline, as was the case at the deep water stations. The vertical distribution of the  $a - a_w(412)/b - b_w(412)$  ratios also changed little with depth and did not increase significantly below the seasonal thermocline. The pattern of the vertical distribution of the values of this ratio indicate that the contribution of soluble material to the absorption budget was not observed in the examples presented. From this, it can be concluded that the settling of particulate material from the riverine plume could be responsible for the elevated values of  $a - a_w(412)$  and  $b - b_w(412)$  in the mixed layers beneath both the plume water lenses and the seasonal thermocline.

The large number of data from depth profiles acquired with the Integrated Optical-Hydrological Probe were used to verify the distribution of CDOM fluorescence intensities and absorption coefficient  $a - a_w(412)$  as a function of salinity. Figure 10 presents the distribution of CDOM fluorescence intensity measured in situ; it includes the  $I_{Fl\_raw}$  (Figure 10a) and  $a - a_w(412)$  coefficient (Figure 10b) as a function of salinity for all the vertical profiles measured during two cruises in September and October 2009. There is a distinct increasing trend in the  $I_{Fl\_raw}$  values with increasing salinity in the 8–12 salinity range, as indicated previously in Figure 7. The distribution of the  $a - a_w(412)$  coefficient as a function of salinity also exhibited small increases in the absorption coefficient with

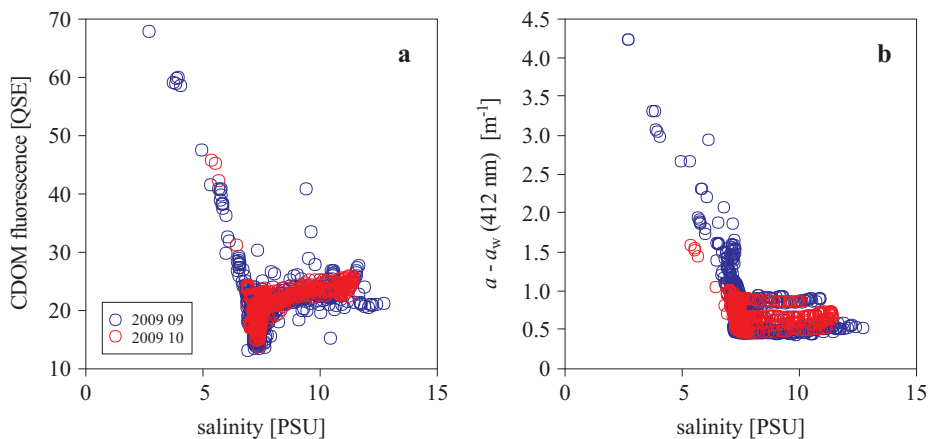


**Figure 10.** Distribution of fluorescence intensity (a) and absorption coefficient less that due to water  $a - a_w(412)$  (b) as a function of salinity. Data acquired using the Integrated Optical-Hydrological Probe during field surveys in September (blue circles) and October (red circles) 2009

increasing salinity in the same salinity range; however, differences between  $a - a_w(412)$  vs. salinity were observed for individual casts. This could have resulted from the variable contribution of soluble and particulate material to the total absorption.

#### 4. Discussion

Fluorescence is a radiometric quantity that can be measured easily in the laboratory, in situ, and from remote sensing platforms. There are reports of lidar systems on various airborne platforms being used for studying the spatial distribution of CDOM fluorescence (Reuter et al. 1986, Hoge et al. 1993a), and of in situ deployments of single channel or multi-channel fluorometers (Conmy et al. 2004, Belzile et al. 2006). The deployment of portable fluorometers for in situ CDOM measurements must take into account the presence of particles in sea water that attenuate excitation and emit light on the path length between the excitation light source, the excited water volume and the emitted light detector. Organic particles, or inorganic particles coated with organic matter films, can also contribute to the emitted light signal. The interference of in situ measurements of CDOM fluorescence by particles was studied by Belzile et al. (2006), who estimated a possible error in fluorescence signal retrieval of less than 4%. The current study was performed within a similar variability range of CDOM optical properties as those reported by Belzile et al. (2006). However, the presence of particles in water can decrease the CDOM fluorescence signal by 35% relative to fluorescence measurements in filtered water. Although the relative difference between the fluorescence intensities measured in raw and filtered water is high, these two quantities are very well correlated, and correction factors can be applied based on empirical calibration. The empirical relationships between fluorescence intensities measured in raw and filtered water presented in the current study cannot be transferred easily to other water bodies because the composition of the soluble organic compounds comprising CDOM could be different; thus, the apparent quantum yield of CDOM fluorescence could also be different. Therefore, this procedure must be followed each time the fluorometer is deployed in a new environment.

DOM fluorescence in natural waters has been used as a proxy for the CDOM absorption coefficient, and results published in numerous reports from a wide range of aquatic environments, including the Baltic Sea, confirm the strong linear relationship between DOM fluorescence and dissolved absorption (e.g. Ferrari & Tassan 1991, Hoge et al. 1993b, Green & Blough 1994, Vodacek et al. 1995, Ferrari & Dowell 1998, Ferrari 2000, Chen et al. 2002, Kowalczyk et al. 2003, Del Vecchio & Blough 2004). Typically,

the CDOM absorption coefficient at excitation wavelengths (usually around 350 nm) is correlated with the integrated fluorescence signal normalized to water Raman scattering peaks (and sometimes standardized to quinine sulphate equivalents (QSE in ppb)) and are measured in collected and processed water samples with bench-top fluorimeters. Published empirical relationships between the CDOM absorption coefficient and fluorescence intensity are derived from results of field data collected from various coastal, marine and estuarine environments in Europe, the American Atlantic and Pacific coasts (the published determination coefficients are usually higher than 0.9). The relationships between  $a_{\text{CDOM}(370)}$ ,  $I_{\text{Fl\_raw}}$  and  $I_{\text{Fl\_filtered}}$  presented in the current study can be regarded as linear within the range of variability given here, and the values of the correlation coefficients were above 0.9 while those of the determination coefficients were slightly less than 0.9. The values of  $R$  and  $R^2$  obtained in the current work are smaller than those reported by Ferrari & Dowell (1998); they were calculated for approximately the same sample size and seasonal distribution of samples collected. The only difference is that Ferrari & Dowell (1998) measured fluorescence using a bench-top spectrofluorometer. The current study indicates that there is significant seasonal variation in the regression coefficient between the CDOM absorption coefficient and CDOM fluorescence intensities. The regression coefficient values describing the slope and intercept of the linear relationship do not differ considerably in spring or summer but increase significantly in winter. In the previous work, Ferrari & Dowell (1998) reported seasonal variation in the CDOM fluorescence quantum yield (with the highest values in spring and the lowest at the end of summer), but the reported seasonal variability in regression coefficients calculated for the linear relationship between the CDOM absorption coefficient and fluorescence intensities was relatively small. The present results may well tally with the findings by Ferrari & Dowell (1998); however, direct comparisons are not possible since these authors did not include any data from the cold part of the year (autumn and winter).

In coastal areas where there is a significant supply of allochthonous organic matter from the land, and both CDOM optical properties and DOC concentration behave conservatively at local scales, it is possible to estimate DOC concentration with CDOM absorption, and a statistically significant correlation between CDOM optical properties and Dissolved Organic Carbon is usually observed. Based on these assumptions, relationships between CDOM optical properties and DOC concentration have been studied in various waters for the last three decades. There are numerous reports that indicate empirical relationships between CDOM

optical properties and DOC concentrations in many coastal areas dominated by riverine discharge with statistically significant regression coefficients and high correlation coefficients (e.g. Nyquist 1979, Vodacek et al. 1995, Ferrari et al. 1996, Del Castillo et al. 1999). However, later publications indicate that the optical properties of CDOM are not conservative: they change because of CDOM degradation processes such as photochemical reactions and bacterial grazing, which also lead to seasonal variability in  $a_{\text{CDOM}}(\lambda)$  vs. DOC relationships in the coastal waters of oceans (Vodacek et al. 1997, Rochelle-Newall & Fisher 2002a, Del Vecchio & Blough 2004, Mannino et al. 2008). The data collected during the current study demonstrate that, despite the seasonal variation in linear relationships between  $a_{\text{CDOM}}(370)$ , fluorescence intensities and DOC concentrations, they can be used to observe DOC dynamics with reasonable accuracy. The correlation coefficients for the linear regression between  $a_{\text{CDOM}}(370)$  and DOC were lower in value than those presented by Ferrari et al. (1996); in the current study the relationships derived were based on a much larger data set, which covered two seasonal cycles and have a much broader temporal distribution (data from autumn and winter are included).

The optically inactive fraction of DOC (both non-absorbing and non-fluorescent) is very high in the Baltic Sea, comprising an average of almost 62.5% of the total DOC fraction. The non-absorbing DOC fraction calculated from the inversion of linear regression equations for all the relationships analysed was within the 230–280  $\mu\text{M C}$  range, depending on the season and the parameters used in the regression analysis. This is the same range of magnitude as that presented by Ferrari et al. (1996) (LTO method for DOC estimation). The average concentration of non-absorbing DOC is about three times higher than that reported in other oceanic coastal regions where the concentration of non-absorbing DOC is within the 50–100  $\mu\text{M C}$  range (Vodacek et al. 1997, Rochelle-Newall & Fisher 2002a, Del Vecchio & Blough 2004, Mannino et al. 2008). Similarly high values of the non-absorbing DOC fraction are reported by Ferrari (2000) for the  $a_{\text{CDOM}}(355)$  vs. DOC concentration in the Rhine river plume. The current data indicate that higher optically inactive DOC concentrations are observed in spring with a decrease towards the end of summer. This concurs well with data presented in reports from the USA Atlantic coast (Vodacek et al. 1997, Rochelle-Newall & Fisher 2002a, Del Vecchio & Blough 2004, Mannino et al. 2008), where the non-absorbing DOC fraction decreased in the mixing zone from about 80–90  $\mu\text{M C}$  in spring to around 50  $\mu\text{M C}$  in summer.

The carbon-specific CDOM absorption coefficients reported in this study were compared with those published in the literature after the conversion

of DOC concentration units (from  $\mu\text{M C}$  into  $\text{g m}^{-3}$ ) and the spectral adjustment of the CDOM absorption coefficient. The average value and standard deviation of the carbon-specific CDOM absorption coefficient  $a^*_{\text{CDOM}}(370)$  was  $0.0044 \pm 0.00202 \text{ m}^2 \text{ mM}^{-1}$  (for comparison with other studies, the average and SD values of the  $a^*_{\text{CDOM}}(350) = 0.00662 \pm 0.00202 \text{ m}^2 \text{ mM}^{-1}$  are also presented). The average value of  $a^*_{\text{CDOM}}(370)$  was in the middle of the variability range reported for the carbon-specific CDOM absorption coefficients in Delaware and Chesapeake Bays on the east coast of the USA, and it was at least three times higher than typical values of this parameter noted in Atlantic coastal waters (Del Vecchio & Blough 2004). The minimum values of  $a^*_{\text{CDOM}}(370)$  were almost twice as high as those reported by Del Vecchio & Blough (2004) in the Mid-Atlantic Bight. The values of  $a^*_{\text{CDOM}}(370)$  from the upper end of the variability range were lower than those reported for terrestrial CDOM end members noted in estuarine waters (e.g. Kowalczyk et al. 2010). Values of the carbon-specific CDOM absorption coefficient observed in the Baltic Sea were also compared with those published by Carder et al. (1989) for fulvic and humic acids isolated from waters of the Gulf of Mexico. The lowest value of  $a^*_{\text{CDOM}}(450)$  (in  $\text{m}^2 \text{ g}^{-1}$ ) in the current data set is an order of magnitude higher than the  $a^*_{\text{CDOM}}(450)$  value for isolated fulvic acids. Although of the same order of magnitude, the highest values of  $a^*_{\text{CDOM}}(450)$  in the current data set were close to values of the same parameter reported for isolated humic acids in the Gulf of Mexico. They were lower than the same values for specific absorption coefficients estimated for humic acids extracted from soils (Zepp & Schlotzhauer 1981), and  $a^*_{\text{CDOM}}(370)$  was found to be almost invariant with season. A similar phenomenon is reported by Del Vecchio & Blough (2004), who noted the stable seasonal distribution of  $a^*_{\text{CDOM}}(355)$  in the Mid-Atlantic Bight.

The  $a^*_{\text{CDOM}}(370)$  values increased with increasing values of  $a_{\text{CDOM}}(370)$ . The same trend was observed in the distribution of  $I_{\text{Fl}_{\text{raw}}}/\text{DOC}$  and  $I_{\text{Fl}_{\text{filtered}}}/\text{DOC}$  as in the function of  $I_{\text{Fl}_{\text{raw}}}$  and  $I_{\text{Fl}_{\text{filtered}}}$  respectively. The approximation of this trend used in the hyperbolic function was very good with  $R^2 = 0.91$  in both instances. The hyperbolic approximation of the carbon-specific CDOM absorption and fluorescence intensity are presented in Kowalczyk et al. (2010) for the South Atlantic Bight, and they are plotted in Figure 6b for comparison. From the comparison of the distribution of  $a^*_{\text{CDOM}}(350)$  vs.  $a_{\text{CDOM}}(350)$  in the Baltic Sea and the South Atlantic Bight one may infer that Baltic Sea DOM has much lower values of the carbon-specific CDOM absorption coefficient per absorption unit than that of the South Atlantic Bight. This could be explained by the very high contribution (nearly 63%) of non-absorbing DOC to the total DOC concentration in



the Baltic Sea. The similar functional shape of the distribution of carbon-specific DOM absorption and fluorescence intensity observed in both regions leads to the conclusion that the hyperbolic relationship could be a universal function applicable in the modelling of  $a^*_{\text{CDOM}}(\lambda)$  and  $I_{\text{F1}}/\text{DOC}$  values in different coastal regions. The regression coefficient derived for hyperbolic approximations may be unique to a specific region; this will depend on the composition and individual contributions of the different water-soluble organics that comprise CDOM, and determine its bulk optical properties. The composition of the heterogeneous mixture of soluble organic compounds in the water depends on the quality and quantity of the precursory organic material comprising CDOM and its transformation in the aquatic environment through photochemical and bacterial reworking. To date, only a few reports have been published that provide information on the impact CDOM composition has on specific optical properties. The classic work by Carder et al. (1989) presents evidence that the carbon-specific absorption coefficient of the fulvic fraction of marine humus substances increased with increasing molecular weight, while the carbon-specific absorption coefficient of the humic fraction of the marine humus substances decreased with increasing molecular weight. They also proposed a model for calculating the bulk optical properties of CDOM based on the fulvic fraction, defined as the ratio between the concentrations of fulvic and humic acids. The extraction procedures and chemical analysis needed to calculate the concentrations of both fractions of humus substances in the marine environment are very difficult and extremely time consuming; therefore, the Carder et al. (1989) model was derived from a limited data base compiled from field observations. Fluorescence spectroscopy is a relatively simple and cost-efficient method for rapidly characterizing DOM composition. On the basis of DOM fluorescence Excitation and Emission Matrix data collected in the South Atlantic Bight, Kowalczyk et al. (2010) put forward a simple statistical model that explains the variation in  $a^*_{\text{CDOM}}(350)$  with changes in the fluorescence intensity ratios of specific DOM components derived from the PARAFAC model. They found that  $a^*_{\text{CDOM}}(350)$  values are largely controlled by the ratios of terrestrial humic-like components and protein-like components.

The bulk of DOC concentrations and their specific optical properties in the surface water of the Baltic Sea are controlled mainly by the inflow of dissolved organic matter from the land by rivers and its mixing with marine waters. The linear approximation of this process explains at least 80% of the variability in  $a_{\text{CDOM}}(370)$  values, and 90% of that in fluorescence intensity. This agrees very well with the model by Kowalczyk et al. (2006) that predicts  $a_{\text{CDOM}}(375)$  based on season, salinity and chlorophyll *a* concentration. According to the results of this model, mixing is the most

important driver of  $a_{\text{CDOM}}(375)$  variability; however, the contribution of chlorophyll *a* is important in summer during strong thermal stratification, especially in areas that are not under the direct influence of riverine plumes. Samples from the spring season, when riverine inflow into the Baltic Sea is at its maximum and thermal stratification is rather weak, are the most numerous in the current data set. This could explain the excellent relationships of the CDOM absorption coefficient and fluorescence intensity with salinity. The DOC concentration reported in the current paper is within the range of DOC variability reported by Kuliński & Pempkowiak (2008, and the references therein). The primary source of organic carbon in the Baltic Sea is the input of terrestrial Dissolved Organic Matter discharged to this region with riverine waters (Pempkowiak & Kupryszewski 1980), and this could explain the high proportion of optically inactive DOC in the total DOC concentration. The current data suggest that the mixing of terrestrial DOC in the marine environment explains just 61% of the DOC concentration variability in the study area. Kuliński & Pempkowiak (2008) propose a model that estimates DOC variability in the southern Baltic Sea in spring based on organic matter derived from river runoff and zooplankton activity as well as that released from phytoplankton cells. Their model explains 78% of the variability in the DOC pool, which indicates that other sources and sinks of DOC must be taken in to account, for example, the flocculation of riverine DOM in the salinity gradient at the hydrological front (Grzybowski & Pempkowiak 2003), photochemical degradation (Grzybowski 2000 and 2002) and bacterial uptake (Ochocki et al. 1995).

With the Integrated Optical-Hydrological Probe used to acquire high-resolution vertical profiles of inherent optical properties, temperature, salinity and CDOM fluorescence enabled the measurable effects of some processes influencing DOC distributions in different layers in Baltic Sea waters to be recorded. The depletion of the fluorescence intensity in the upper mixing zone (see Figure 8) could be regarded as evidence for the photochemical decomposition of DOM and possible DOC mineralization in the mixing zone above the seasonal thermocline in open Baltic Sea waters. This effect would not be apparent with  $a_{\text{c-9}}$  measurements alone because of the masking effect of particulate absorption. Although CDOM plays a dominant role in the absorption budget in the Baltic Sea (Kowalczyk & Darecki 1998) and could contribute up to 80% of the total absorption coefficient in blue light, the absorption coefficient  $a - a_w(412)$  cannot be regarded as an approximate proxy of  $a_{\text{CDOM}}(\lambda)$  because the contribution of CDOM absorption to the total absorption is temporally and spatially variable. Simultaneous measurements of the spectral absorption coefficient

and fluorescence intensity, together with the derived empirical relationship between  $a_{\text{CDOM}}(370)$  and  $I_{\text{Fl}_{\text{raw}}}$  should enable the partitioning of the  $a - a_w(\lambda)$  coefficient into the contributions of the major optically significant sea water constituents to the total absorption coefficient. This could also be achieved with simultaneous casts of two ac-9 instruments, one equipped with  $0.2 \mu\text{m}$  maxicapule filters attached to the water intake and one without filters. This method was applied successfully by Boss et al. (2001) and Twardowski & Donaghay (2002) in measurements of spatial and temporal variations in the absorption of dissolved material in the Atlantic and Pacific Oceans off the east and west coasts of the USA. Twardowski & Donaghay (2002) also report the effect of CDOM photodegradation in the mixed layer based on direct in situ measurements and put forward a statistical model to quantify this effect. This approach is not readily applicable in Baltic Sea waters, however, because of the high concentrations of suspended solids that clog filters.

Qualitative analysis of the vertical profiles of the inherent optical properties and physical properties of sea water acquired with the Integrated Optical-Hydrological Probe also permitted a significant source of DOC to be identified in deep Baltic Sea waters below the permanent pycnocline. It is unlikely that DOC was transported along with these water masses originating from the North Sea. DOC measurements in the current data base obtained in the Skagerrak and Kattegat indicate that concentrations seldom exceeded  $200 \mu\text{M C}$ , which is the baseline concentration in the Baltic Sea. It is very likely that elevated DOC concentrations in Baltic Sea deeps are produced locally during the bio-chemical or microbial decomposition of particulate material precipitating from the mixed layer. The role of the bacterial production of CDOM has been explained by the conceptual model proposed by Rochelle-Newall & Fisher (2002b). Another source of DOC and optically active DOM in Baltic Sea deeps could be diffusion from bottom sediments. Skoog et al. (1996) report increased fluorescent DOM flux through the sediment-water interface in the deep water of Gullmar Fjord, Sweden, during anoxic conditions. Rochelle-Newall et al. (1999) also observed increased CDOM production in anoxic sediments. Such conditions are very frequent in the Baltic Sea deeps. This conclusion concurs with the recent study by Kuliński (2010), who estimated the return carbon flux from bottom sediments of Baltic Sea deeps to the water column at 25–32% of the organic carbon that is currently deposited there. The majority of this flux is related to inorganic carbon forms; however, from 5% to 9% ( $11.3 \text{ moles DOC m}^{-2} \text{ a}^{-1}$ , on average) of the total return carbon flux could be attributable to DOC.

## 5. Conclusions

Over two years of intensive field surveys, the applicability of a small, commercially-available fluorometer was successfully tested for in situ measurements of CDOM fluorescence intensity. The impact of suspended solids on the measurement accuracy of CDOM fluorescence intensity was assessed, and an empirical formula to correct CDOM fluorescence intensity readings measured in situ to the corresponding CDOM fluorescence intensity values of dissolved organic material was derived. The fluorescence correlated very well with the CDOM absorption coefficient  $a_{\text{CDOM}}(370)$ . Fluorescence can be regarded as a CDOM absorption proxy, and empirical relationships are presented enabling CDOM absorption to be estimated from fluorescence intensities measured in situ. Both fluorescence and the CDOM absorption coefficient correlated well with the DOC concentrations; it was therefore possible to estimate DOC concentrations using optical instrumentation. The variability of the CDOM carbon-specific inherent optical properties is discussed and a statistical model that could be useful for estimating these parameters in the Baltic Sea is proposed. With the use of the Integrated Optical-Hydrological Probe for acquiring high-resolution vertical profiles of inherent optical properties, temperature, salinity and CDOM fluorescence, the effects of CDOM degradation and DOC mineralization in the mixed layer to be recorded and new sources of CDOM and DOC in the deep waters of the Baltic Sea below the permanent pycnocline can be found. The empirical relationships observed between DOC and CDOM optical properties, and the new approach to high spatial resolution measurements of physical and optical properties in Baltic Sea water provide new tools for observing and quantifying DOC dynamics in this environment.

## Acknowledgements

We thank the technical staff, officers and the crew of r/v 'Oceania' for providing logistical support and assistance during the field work.

## References

- Bélanger S., Babin M., Larouche P., 2008, *An empirical ocean color algorithm for estimating the contribution of chromophoric dissolved organic matter to total light absorption in optically complex waters*, J. Geophys. Res., 113, C04027, doi:10.1029/2007JC004436.
- Bélanger S., Xie H., Krotkov N., Larouche P., Vincent W.F., Babin M., 2006, *Photomineralization of terrigenous dissolved organic matter in Arctic coastal waters from 1979 to 2003: Interannual variability and implications of climate change*, Global Biogeochem. Cy., 20 (4), GB4005, doi:10.1029/2006GB002708.

- Belzile C., Roesler C.S., Christensen J.P., Shakhova N., Semiletov I., 2006, *Fluorescence measured using the WETStar DOM fluorometer as a proxy for dissolved matter absorption*, *Estuar. Coast. Shelf Sci.*, 67 (3), 441–449.
- Blough N.V., Del Vecchio R., 2002, *Chromophoric DOM in the coastal environment*, [in:] *Biogeochemistry of marine dissolved organic matter*, D. Hansell & C. Carlson (eds.), Acad. Press, New York, 509–546.
- Boss E., Pegau W.S., Zaneveld J.R., Barnard A.H., 2001, *Spatial and temporal variability of absorption by dissolved material at a continental shelf*, *J. Geophys. Res.*, 106 (C5), 9499–9507.
- Chen R. F., Zhang Y., Vlahos P., Rudnick S. M., 2002, *The fluorescence of dissolved organic matter in the Mid-Atlantic Bight*, *Deep-Sea Res. Pt. II*, 49 (20), 4439–4459.
- Coble P. G., 2007, *Marine optical biogeochemistry: the chemistry of ocean color*, *Chem. Rev.*, 107 (2), 402–418.
- Conmy R. N., Coble P. G., Del Castillo C. E., 2004, *Calibration and performance of a new in situ multi-channel fluorometer for measurement of colored dissolved organic matter in the ocean*, *Cont. Shelf Res.*, 24 (3), 431–442.
- Darecki M., Weeks A., Sagan S., Kowalczyk P., Kaczmarek S., 2003, *Optical characteristics of two contrasting case 2 waters and their influence on remote sensing algorithms*, *Cont. Shelf Res.*, 23 (3–4), 237–250.
- Del Castillo C. E., Coble P. G., Morell J. M., López J. M., Corredor J. E., 1999, *Analysis of the optical properties of the Orinoco River plume by absorption and fluorescence spectroscopy*, *Mar. Chem.*, 66 (1–2), 35–51.
- Del Castillo C. E., Miller R. L., 2008, *On the use of ocean color remote sensing to measure the transport of dissolved organic carbon by the Mississippi River Plume*, *Remote Sens. Environ.*, 112 (3), 836–844.
- Del Vecchio R., Blough N. V., 2004, *Spatial and seasonal distribution of chromophoric dissolved organic matter and dissolved organic carbon in the Middle Atlantic Bight*, *Mar. Chem.*, 89 (1–4), 169–187.
- Del Vecchio R., Subramaniam A., Schollaert Uz S., Ballabrera-Poy J., Brown C. W., Blough N. V., 2009, *Decadal time-series of SeaWiFS retrieved CDOM absorption and estimated CO<sub>2</sub> photoproduction on the continental shelf of the eastern United States*, *Geophys. Res. Lett.*, 36, L02602, doi:10.1029/2008GL036169.
- D'Sa E. J., Miller R. L., 2003, *Bio-optical properties in waters influenced by the Mississippi River during low flow conditions*, *Remote Sens. Environ.*, 84 (4), 538–549.
- Duursma E. K., 1965, *The dissolved organic constituents of seawater*, [in:] *Chemical oceanography*, Vol 1., J. P. Riley & G. Skirrow (eds.), Acad. Press, London, 433–475.
- Ferrari G., 2000, *The relationship between chromophoric dissolved organic matter and dissolved organic carbon in the European Atlantic coastal area and in the West Mediterranean Sea (Gulf of Lions)*, *Mar. Chem.*, 70 (4), 339–357.

- Ferrari G., Dowell M. D., 1998, *CDOM absorption characteristics with relation to fluorescence and salinity in coastal areas of the southern Baltic Sea*, Estuar. Coast. Shelf Sci., 47 (1), 91–105.
- Ferrari G., Dowell M. D., Grossi S., Targa C., 1996, *Relationship between optical properties of chromophoric dissolved organic matter and total concentration of dissolved organic carbon in southern Baltic Sea region*, Mar. Chem., 55 (3–4), 299–316.
- Ferrari G., Tassan S., 1991, *On the accuracy of determining light absorption by 'yellow substance' through measurements of induced fluorescence*, Limnol. Oceanogr., 36 (4), 777–786.
- Fichot C. G., Sathyendranath S., Miller W. L., 2008, *SeaUV and SeaUV(C): Algorithms for the retrieval of UV/visible diffuse attenuation coefficients from ocean color*, Remote Sens. Environ., 112 (4), 1584–1602.
- Garver S. A., Siegel D. A., 1997, *Inherent optical property inversion of ocean color spectra and its biogeochemical interpretation, 1. Time series from the Sargasso Sea*, J. Geophys. Res., 102 (C8), 18607–18625.
- Green S. A., Blough N. V., 1994, *Optical absorption and fluorescence properties of chromophoric dissolved organic matter in natural waters*, Limnol. Oceanogr., 39 (8), 1903–1916.
- Grzybowski W., 2000, *Effect of short-term irradiation on the absorbance spectra of the chromophoric organic matter dissolved in the coastal and riverine waters*, Chemosphere, 40 (12), 1313–1318.
- Grzybowski W., 2002, *The significance of dissolved organic matter photodegradation as a source of ammonium in natural waters*, Oceanologia, 44 (3), 355–365.
- Grzybowski W., Pempkowiak J., 2003, *Preliminary results on low molecular weight organic substances dissolved in the waters of the Gulf of Gdańsk*, Oceanologia, 45 (4), 693–704.
- Hansell D. A., Carlson C. A., 1998, *Deep-ocean gradients in the concentration of dissolved organic carbon*, Nature, 395 (6699), 263–266.
- Hansell D. A., Carlson C. A., 2001, *Marine dissolved organic matter and the carbon cycle*, Oceanography, 14 (4), 41–49.
- Hoge F. E., Swift R. N., Yungel J. K., Vodacek A., 1993a, *Fluorescence of dissolved organic matter: A comparison of North Pacific and North Atlantic Oceans during April 1993*, J. Geophys. Res., 98 (C12), 22 779–22 787.
- Hoge F. E., Vodacek A., Blough N. V., 1993b, *Inherent optical properties of the ocean: retrieval of the absorption coefficient of chromophoric dissolved organic matter from fluorescence measurements*, Limnol. Oceanogr., 38 (7), 1394–1402.
- Højerslev N. K., 1988, *Natural occurrences and optical effects of Gelbstoff*, Rep. No. 50, Inst. Phys. Oceanogr., Univ. Copenhagen, 30 pp.
- Højerslev N. K., 1989, *Surface water quality studies in the interior marine environment of Denmark*, Limnol. Oceanogr., 34 (8), 1630–1639.
- Højerslev N. K., Holt N., Aarup T., 1996, *Optical measurements in the North Sea–Baltic Sea transition zone. 1. On the origin of the deep water in the Kattegat*, Cont. Shelf Res., 16 (10), 1329–4343.

- Jerlov N. G., 1976, *Marine optics*, Elsevier, New York, 231 pp.
- Johannessen S. C., Miller W. L., 2001, *Quantum yield for the photochemical production of dissolved inorganic carbon in seawater*, Mar. Chem., 76 (4), 271–283.
- Johannessen S. C., Miller W. L., Cullen J. J., 2003, *Calculation of UV attenuation and colored dissolved organic matter absorption spectra from measurements of ocean color*, J. Geophys. Res., 108 (C9), 3301, doi:10.1029/2000JC000514.
- Kahru M., Mitchell B. G., 2001, *Seasonal and non-seasonal variability of satellite derived chlorophyll and colored dissolved organic matter concentration in the California Current*, J. Geophys. Res., 106 (C2), 2517–2529.
- Kirk J. T. O., 1994, *Light and photosynthesis in aquatic ecosystems*, 2nd edn., Cambridge Univ. Press, New York, 509 pp.
- Kowalczyk P., 1999, *Seasonal variability of yellow substance absorption in the surface layer of the Baltic Sea*, J. Geophys. Res., 104 (C12), 30047–30058.
- Kowalczyk P., Cooper W. J., Durako M. J., Kahn A. E., Gonsior M., Young H., 2010, *Characterization of dissolved organic matter fluorescence in the South Atlantic Bight with use of PARAFAC model: Relationships between fluorescence and its components, absorption coefficients and organic carbon concentrations*, Mar. Chem., 118 (1–2), 22–36.
- Kowalczyk P., Cooper W. J., Whitehead R. F., Durako M. J., Sheldon W., 2003, *Characterization of CDOM in organic rich river and surrounding coastal ocean in the South Atlantic Bight*, Aquat. Sci., 65 (4), 384–401.
- Kowalczyk P., Darecki M., 1998, *The relative share of light absorption by yellow substances in total light absorption in the surface layer of southern Baltic Sea*, Proc. Ocean Optics XIV Conf., Kailua Kona, Hawaii, USA, 10–13 November 1998, paper 1052, 9 pp.
- Kowalczyk P., Darecki M., Olszewski J., Kaczmarek S., 2005, *Empirical relationships between Coloured Dissolved Organic Matter (CDOM) absorption and apparent optical properties in Baltic Sea waters*, Int. J. Remote Sens., 26 (2), 345–370.
- Kowalczyk P., Kaczmarek S., 1996, *Analysis of temporal and spatial variability of 'yellow substance' absorption in the Southern Baltic*, Oceanologia, 38 (1), 3–32.
- Kowalczyk P., Stedmon C. A., Markager S., 2006, *Modeling absorption by CDOM in the Baltic Sea from season, salinity and chlorophyll*, Mar. Chem., 101 (1–2), 1–11.
- Kuliński K., 2010, *Carbon cycling in the Baltic Sea*, Ph.D. thesis, Inst. Oceanol. PAN, Sopot, 134 pp., (in Polish).
- Kuliński K., Pempkowiak J., 2008, *Dissolved organic carbon in the southern country-region Baltic Sea: Quantification of factors affecting its distribution*, Estuar. Coast. Shelf Sci., 78 (1), 38–44.
- Mannino A., Russ M. E., Hooker S. B., 2008, *Algorithm development and validation for satellite-derived distributions of DOC and CDOM in the U.S. Middle Atlantic Bight*, J. Geophys. Res., 113, C07051, doi:10.1029/2007JC004493.

- Maritorena S., Siegel D. A., Peterson A. R., 2002, *Optimization of a semi-analytical ocean color model for global-scale applications*, Appl. Optics, 41 (15), 2705–2714.
- Morel A., Prieur L., 1977, *Analysis in variation of ocean color*, Limnol. Oceanogr., 22 (4), 709–722.
- Nelson N. B., Siegel D. A., Carlson C. A., Swan C., Smethie Jr. W. M., Khatiwala S., 2007, *Hydrography of chromophoric dissolved organic matter in the North Atlantic*, Deep-Sea Res. Pt. I, 54 (5), 710–731.
- Nyquist G., 1979, *Investigation of some optical properties of sea water with special reference to lignin sulphates and humic substances*, Ph.D. thesis, Dpt. Anal. Mar. Chem., Göteborg Univ., Göteborg, 203 pp.
- Ochocki S., Nakonieczny J., Chmielowski H., Zalewski M., 1995, *The hydrochemical and biological impact of the river Vistula on the pelagic system of the Gulf of Gdańsk in 1994. Part 2. Primary production and chlorophyll a*, Oceanologia, 37 (2), 207–226.
- Olszewski J., Sagan S., Darecki M., 1992, *Spatial and temporal changes in some optical parameters in the southern Baltic*, Oceanologia, 33, 87–103.
- Pempkowiak J., Kupryszewski G., 1980, *The input of organic matter to the Baltic from the Vistula River*, Oceanologia, 12, 79–98.
- Rochelle-Newall E. J., Fisher T. R., 2002a, *Chromophoric dissolved organic matter and dissolved organic carbon in Chesapeake Bay*, Mar. Chem., 77 (1), 23–41.
- Rochelle-Newall E. J., Fisher T. R., 2002b, *Production of chromophoric dissolved organic matter fluorescence in marine and estuarine environments: an investigation into the role of phytoplankton*, Mar. Chem., 77 (1), 7–21.
- Rochelle-Newall E. J., Fisher T. R., Fan C. L., Glibert P. M., 1999, *Dynamics of chromophoric dissolved organic matter and dissolved organic carbon in experimental mesocosms*, Int. J. Remote Sens., 20 (3), 627–641.
- Reuter R., Diebel-Langohr D., Dörre F., Hengstermann T., 1986, *Airborne laser fluorosensor measurements of Gelbstoff, [in:] The influence of yellow substances on remote sensing of sea water constituents from space*, Rep. ESA Contract RFQ 3-5060/84/NL/MD, GKSS Res. Cent., Geesthacht, Germany.
- Sagan S., 1991, *Light transmission in the water of the southern Baltic Sea*, Diss. Monogr. 2, Inst. Oceanol. PAN, Sopot, 137 pp., (in Polish).
- Sathyendranath S. (ed.), 2000, *Remote sensing of ocean colour in coastal, and other optically-complex, waters*, IOCCG Rep. No. 3, Dartmouth, CA, 140 pp.
- Siegel D. A., Maritorena S., Nelson N. B., Behrenfeld M. J., 2005a, *Independence and interdependencies among global ocean color properties: Reassessing the bio-optical assumption*, J. Geophys. Res., 110, C07011, doi:10.1029/2004JC002527.
- Siegel D. A., Maritorena S., Nelson N. B., Behrenfeld M. J., McClain C. R., 2005b, *Colored dissolved organic matter and its influence on the satellite-based characterization of the ocean biosphere*, Geophys. Res. Lett., 32, L20605, doi:10.1029/2005GL024310.



- Siegel D. A., Maritorena S., Nelson N. B., Hansell D. A., Lorenzi-Kayser M., 2002, *Global distribution and dynamics of colored dissolved and detrital organic materials*, J. Geophys. Res., 107 (C12), 3228, doi:10.1029/2001JC000965.
- Shank G. C., Zepp R. G., Whitehead R. F., Moran M. A., 2005, *Variations in the spectral properties of freshwater and estuarine CDOM caused by partitioning onto river and estuarine sediments*, Estuar. Coast. Shelf Sci., 65 (1–2), 289–301.
- Sharp J. H., 2002, *Analytical methods for total DOM pools*, [in:] *Biogeochemistry of marine dissolved organic matter*, D. A. Hansell & C. A. Carlson (eds.), Acad. Press, San Diego, CA, 35–58.
- Skoog A., Hall P. O. J., Hulth S., Paxeus N., van der Loeff M. R., Westerlund S., 1996, *Early diagenetic production and sediment–water exchange of fluorescent dissolved organic matter in the coastal environment*, Geochim. Cosmochim. Ac., 60 (19), 3619–3629.
- Skoog A., Wedborg M., Fogelqvist E., 2010, *Organic carbon concentrations and humic substance fluorescence in the Baltic Sea, Kattegatt, and Skagerrak*, Mar. Chem., (in revision).
- Stedmon C. A., Markager S., Kaas H., 2000, *Optical properties and signatures of chromophoric dissolved organic matter (CDOM) in Danish coastal waters*, Estuar. Coast. Shelf Sci., 51 (2), 267–278.
- Stedmon C. A., Osburn C. L., Kragh T., 2010, *Tracing water mass mixing in the Baltic–North Sea transition zone using the optical properties of coloured dissolved organic matter*, Estuar. Coast. Shelf Sci., 87 (1), 156–162.
- Twardowski M. S., Donaghay P. L., 2001, *Separating in situ and terrigenous sources of absorption by dissolved organic materials in coastal waters*, J. Geophys. Res., 106(C7), 2545–2560.
- Vodacek A., Blough N. V., DeGrandpre M. D., Peltzer E. T., Nelson R. K., 1997, *Seasonal variation of CDOM and DOC in the Middle Atlantic Bight: terrestrial inputs and photooxidation*, Limnol. Oceanogr., 42 (2), 674–686.
- Vodacek A., Hoge F., Swift R. N., Yungel J. K., Peltzer E. T., Blough N. V., 1995, *The use of in situ and airborne fluorescence measurements to determine UV absorption coefficients and DOC concentrations in surface waters*, Limnol. Oceanogr., 40 (2), 411–415.
- Woźniak B., Dera J., 2007, *Light absorption in sea water*, Springer, Dordrecht, 456 pp.
- Zaneveld J. R. V., Kitchen J. C., Moore C., 1994, *The scattering error correction of reflecting-tube absorption meters*, Ocean Optics XII, Proc. SPIE, 2258, 44–55.
- Zepp R., Schlotzhauer P. F., 1981, *Comparison of photochemical behaviour of various humic substances in water: 3. Spectroscopic properties of humic substances*, Chemosphere, 10 (5), 479–486.